


Methane cold seeps as biological oases in the high-Arctic deep sea

Emmelie K. L. Åström ^{1*} Michael L. Carroll,^{1,2} William G. Ambrose, Jr.,^{1,2,3,4} Arunima Sen,¹
Anna Silyakova,¹ JoLynn Carroll^{1,2}

¹CAGE - Centre for Arctic Gas Hydrate, Environment and Climate, Department of Geosciences, UiT The Arctic University of Norway, Tromsø, Norway

²Akvaplan-niva, FRAM – High North Research Centre for Climate and the Environment, Tromsø, Norway

³Division of Polar Programs, National Science Foundation, Arlington, Virginia

⁴Department of Biology, Bates College, Lewiston, Maine

Abstract

Cold seeps can support unique faunal communities via chemosynthetic interactions fueled by seabed emissions of hydrocarbons. Additionally, cold seeps can enhance habitat complexity at the deep seafloor through the accretion of methane derived authigenic carbonates (MDAC). We examined infaunal and megafaunal community structure at high-Arctic cold seeps through analyses of benthic samples and seafloor photographs from pockmarks exhibiting highly elevated methane concentrations in sediments and the water column at Vestnesa Ridge (VR), Svalbard (79° N). Infaunal biomass and abundance were five times higher, species richness was 2.5 times higher and diversity was 1.5 times higher at methane-rich Vestnesa compared to a nearby control region. Seabed photos reveal different faunal associations inside, at the edge, and outside Vestnesa pockmarks. Brittle stars were the most common megafauna occurring on the soft bottom plains outside pockmarks. Microbial mats, chemosymbiotic siboglinid worms, and carbonate outcrops were prominent features inside the pockmarks, and high trophic-level predators aggregated around these features. Our faunal data, visual observations, and measurements of sediment characteristics indicate that methane is a key environmental driver of the biological system at VR. We suggest that chemoautotrophic production enhances infaunal diversity, abundance, and biomass at the seep while MDAC create a heterogeneous deep-sea habitat leading to aggregation of heterotrophic, conventional megafauna. Through this combination of rich infaunal and megafaunal associations, the cold seeps of VR are benthic oases compared to the surrounding high-Arctic deep sea.

Highlights

- Seafloor methane emissions support a rich and diverse infaunal community distinct from a nearby non-seepage region
- Megafaunal composition varies significantly along a spatial gradient from inside pockmarks with strong methane emissions toward conventional habitats outside pockmarks
- Methane emissions provide both heterogeneous seabed substrates and enhanced chemosynthetic-based organic matter production

Introduction

Marine environments in the high-Arctic are characterized by intense seasonality, sub-zero bottom water temperatures, and extended periods of overlying sea ice. These polar features set a framework for regulation of communities and ecosystems, with intense, episodic pulses of fresh organic matter interspersed among long periods of food limitation (Carroll et al. 2008; Wassmann and Reigstad 2011; Boetius et al. 2013; Meyer et al. 2013). The deep sea (bathypelagic zone > 1000 m depth) also experiences a framework of food limitation, where photosynthetically derived organic matter (e.g., particulate organic matter, marine snow, fecal pellets) from the euphotic zone has been extensively processed during its transit through the water column, arriving at the seafloor highly degraded (Southward and Southward 1982; Graf 1989; Gage and Tyler 1991). These processes lead to what has been termed a biological desert with respect to macrofaunal and megafaunal communities, with low abundance and biomass, but with sometimes high species diversity

*Correspondence: emmelie.k.astrom@uit.no

Additional Supporting Information may be found in the online version of this article.

This is an open access article under the terms of the Creative Commons Attribution License, which permits use, distribution and reproduction in any medium, provided the original work is properly cited.

(Sanders and Hessler 1969; Rex 1981). Instead, deep-sea benthic communities are usually dominated by meiofauna (< 0.5 mm) (Clough et al. 1997; Vanreusel et al. 2000; Hoste et al. 2007), with microbial activity playing a substantial role in carbon processing and remineralization (Wheeler et al. 1996; Boetius et al. 2013).

The composition of deep-sea benthos is also regulated by factors including sediment characteristics and heterogeneity at the seabed (Etter and Grassle 1992; Carney 2005). The expansive, relatively featureless, soft-bottom plains prevalent in deep-sea environments favor suspension and detrital feeders while at the same time largely excludes epifauna that require hard substrate (Levin et al. 2001; Carney 2005). Habitats with mixed substrates, with a high heterogeneity containing a mosaic of soft and hard bottom, generally support the highest diversity and biomass of benthic communities (Gage and Tyler 1991; Quéric and Soltwedel 2007; Buhl-Mortensen et al. 2012).

Cold seeps are environments where emissions of methane, sulfide, or other reduced chemicals occur at the seafloor and these are known from both deep sea and shallow ocean shelves worldwide (Vanreusel et al. 2009; Olu et al. 2010; Levin et al. 2016). Cold seeps are commonly associated with seafloor features like pockmarks, craters, carbonate mounds, or underwater pingos (Dando et al. 1991; Lammers et al. 1995; Hovland and Svendsen 2006; Ritt et al. 2011; Zeppilli et al. 2012). Pockmarks are circular depressions, formed where upward seepage of gas causes a collapse of sediment, and are common features where gas pockets are present in near-surface sediments (Cathles et al. 2010). Long-term seepage of methane can be accompanied by the precipitation of methane derived authigenic carbonates (MDAC) (Bohrmann et al. 1998; Hovland et al. 2005), leading to sometimes extensive outcrops of MDAC in the vicinity of cold seeps (Vanreusel et al. 2009; Bowden et al. 2013). These combinations of features result in seafloor habitat heterogeneity fundamentally different from the predominant monotypic soft-bottom environment in the deep sea (Rex 1981).

Cold seeps, in general, exhibit a wide range of seep fauna, i.e., chemo-obligate species (Cordes et al. 2010; Levin et al. 2016), and usually support macrofaunal communities with high abundances and biomass but low diversity compared to surrounding non-seep habitats (Levin 2005; Tarasov et al. 2005). Seep-associated organisms may rely directly (chemoautotrophic symbionts) or indirectly (trophic relationships) on anaerobic oxidation of methane (AOM) and sulfate reduction as an alternative energy source, instead of, or in addition to, photoautotrophy (Levin and Michener 2002; Boetius and Suess 2004; Levin 2005; Niemann et al. 2013; Thurber et al. 2013). Habitat heterogeneity and chemosymbiotic foundation species associated with cold seep environments (e.g., siboglinid tubeworms, clams, and mussels) may attract epifauna and vagrant mobile organisms from surrounding habitats, and thereby increase the local diversity of these deep-sea ecosystems (Sellanes et al. 2008; Levin et al. 2016).

Few studies document macrobenthic communities at seeps in polar regions (i.e., Domack et al. 2005; Decker et al. 2012; Åström et al. 2016). One of the most well-studied deep cold seep and chemosynthetic systems within the Arctic is the Håkon Mosby mud volcano (HMMV) located at the border to the Barents Sea (72° N, 14° E) at 1250 m water depth (Vogt et al. 1997; Lein et al. 1999). HMMV has been a focus of biogeochemical and geophysical studies documenting the fate of venting methane from the seabed (Milkov et al. 1999; Lösekann et al. 2008; Decker et al. 2012). The benthic environment around the caldera of HMMV consists of three main habitats; microbial mats, siboglinid (pogonophoran) worm fields and plain light-colored sediments, each possessing different faunal community patterns influenced by seafloor methane emissions (Gebruk et al. 2003; Rybakova et al. 2013). Megafaunal densities and taxa richness varied significantly in relation to these different habitats, (Rybakova et al. 2013) and methane derived carbon is incorporated into the faunal communities via trophic interactions (Gebruk et al. 2003; Decker et al. 2012). Åström et al. (2016) described macrofaunal benthic communities associated with cold seeps around western Svalbard and the northwest Barents Sea shelf (75–79° N). They found distinct seep associated faunal assemblages, novel bivalve species (Åström et al. 2017), and higher biomass at seeps compared to nearby non-seep areas, but with highly localized effects reflecting strong environmental gradients associated with individual seeps.

Discoveries of extensive methane seepage areas around the high-Arctic Svalbard archipelago have been described both from shallow ocean shelves (Solheim and Elverhøi 1993; Westbrook et al. 2009) and from the deep sea (Vogt et al. 1994; Hustoft et al. 2009). Of particular focus in the present context is an active methane venting region at the Vestnesa Ridge (VR), along the continental slope in Fram Strait at 79° N and >1200 m water depth. Numerous pockmarks along this ridge are associated with sub-seabed methane hydrate reservoirs (Vogt et al. 1994; Bünz et al. 2012; Plaza-Faverola et al. 2015) and origin of the gas is both microbial and abiotic/thermogenic (Johnson et al. 2015). Plaza-Faverola et al. (2015) documented the history of methane seepage for the last ~ 2.7 My along VR identifying multiple historical events of seepage. There have also been methane seepage events identified in the stratigraphic record through analysis of fossil marine fauna (Ambrose et al. 2015; Szttybor and Rasmussen 2016). Hong et al. (2016) document vigorous biogeochemical processing and transformations in the surface sediments at VR consistent with high methane consumption via microbial AOM. There has not, however, been a previous formal study of the distribution and abundance of benthic organisms at methane-rich deep-sea pockmarks at such northerly latitudes.

We investigated faunal community patterns of active cold seeps in pockmarks at VR, focusing on infaunal and megafaunal assemblages. We assessed species associations, ecological structure, and diversity of macrofauna by comparing deep-sea

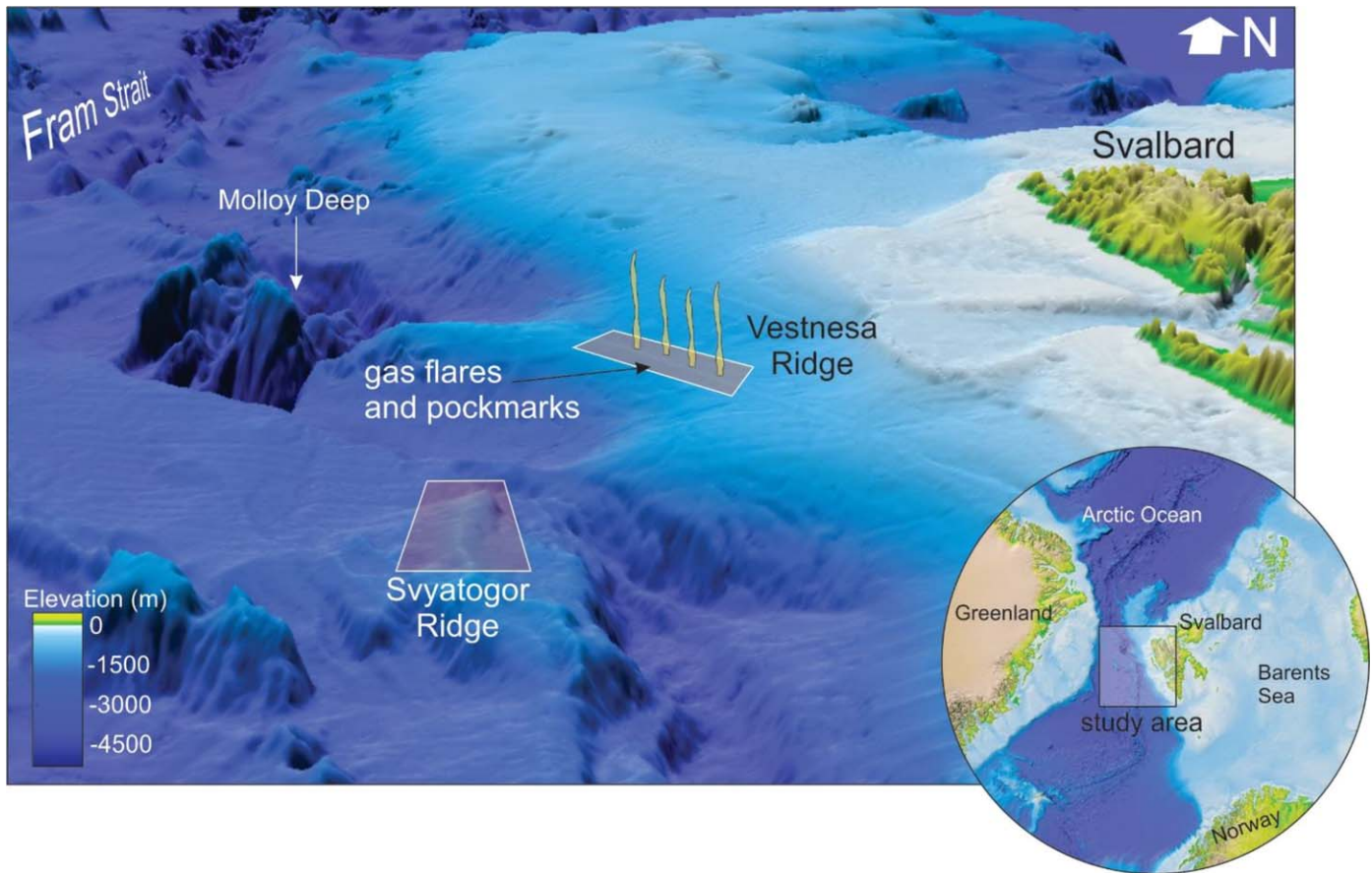


Fig. 1. Map of the sampling region in Western Svalbard showing the active seeping site at VR and the inactive control at SvR. Fram Strait bathymetry is from IBCAO v.3 from Jakobsson et al. (2012).

infaunal samples, sediment characteristics, and methane concentrations at active seeps and a nearby inactive region. In addition to infaunal communities, we describe benthic megafaunal composition associated with pockmarks from VR from analyses of seafloor images. By combining results of analyses from infaunal and megafaunal communities, this study provides new insights into faunal community patterns in a high-Arctic deep-sea methane seep.

Material and methods

Study regions

In order to distinguish between cold seep and conventional deep-sea benthic infaunal communities, we compared an active cold seep region, VR, and an adjacent inactive control region, Svyatogor Ridge (SvR) in the Fram Strait. Both regions are located in the high-Arctic Svalbard archipelago (76–81° N latitude) at the northeastern North Atlantic continental shelf margin (Fig. 1). The Fram Strait is the opening between Greenland and Svalbard and it is the main passage for the exchange of both intermediate and deep-sea water between the Arctic and North Atlantic (Rudels et al. 2000).

VR (Fig. 1), is an approximately 100 km long ultraslow spreading sediment-drift ridge, (79° N, > 1200 m water

depth) (Johnson et al. 2015) located south of the Yermak Plateau and north of the Molly transform fault. We investigated two pockmarks at Vestnesa, both with infaunal benthic sampling and with seafloor imagery (Fig. 2). The pockmarks are approximately 500 m wide or long and around 10–15 m deep and named “Lomvi” and “Lunde” (Fig. 2). Multiple methane bubble plumes have been acoustically detected in the water column above the pockmarks rising up to 800 m above the seafloor (Bünz et al. 2012). Both pockmarks support MDAC outcrops precipitated at the seafloor. These are rock-like formations coupled to the presence of methane and gas hydrates in the sediment (Bohrmann et al. 1998; Crémière et al. 2016).

Approximately 80 km south of VR, another ridge complex, SvR (78° N) (Fig. 1), is located on the northwestern tip of the Knipovich Ridge. VR and SvR once belonged to the same ridge complex, before being separated by the Molloy transform fault (Johnson et al. 2015). Seismic profiles at SvR indicate paleo-seep features including chimneys (acoustic blankings), pockmarks, and sub-surface gas, but no active venting of methane or hydro acoustic plumes have been observed from the region.

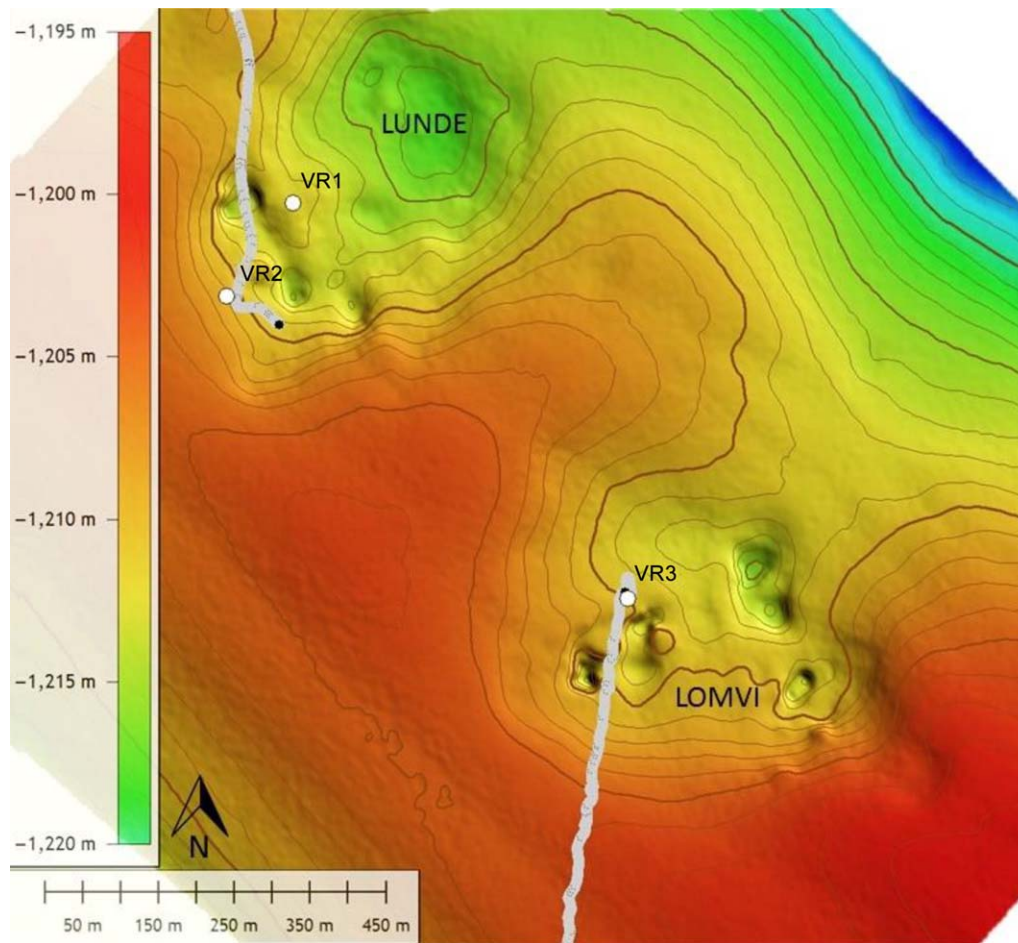


Fig. 2. Seafloor map at VR from depth-converted high-resolution 3D seismic data showing the bathymetry and features of the investigated methane seeping pockmarks. Water depths are approximately 1200 m (color bar). The seismic data were converted from two-way travel time to depth using a water column velocity of 1470 m s^{-1} , as documented from CTD data. Stations sampled for infauna are indicated as white dots and Tow-cam photo transects are shown as gray lines.

Benthic sampling

We sampled the benthos at the two active seeping pockmarks, Lunde and Lomvi, on VR and at the inactive control region, SvR (Figs. 1, 2; Table 1) in June 2014 and May 2015 aboard the RV *Helmer Hanssen*. Range finding and bathymetry were conducted with ship-mounted multi-beam and three-dimensional (3D) seismic surveys. Locations of active hydrocarbon seepages were selected based on acoustic reflections from flares detected on a keel mounted single beam echo sounder (Simrad EK 60 frequencies 18 KHz and 38 KHz) and on information from previous geophysical surveys in the region (Bünz et al. 2012; Smith et al. 2014; Plaza-Faverola et al. 2015). Benthic sampling in 2014 at SvR and VR was conducted using a multicorer ($\varnothing 10 \text{ cm}$) or by subcoring ($\varnothing 10 \text{ cm}$) from a box core. Sampling in 2015 at VR was carried out where characteristic seep features such as flares, microbial mats, and MDAC (hereafter referred to as carbonate outcrops) were identified through seafloor imagery. Images were

captured with a Tow Cam, a camera guided multicorer (cores $\varnothing 10 \text{ cm}$) and conductivity, temperature, depth (CTD) sampler. This towed camera system was developed through Multi-disciplinary Instrumentation in Support of Oceanography (MISO) at Woods Hole Oceanographic Institution (<http://www.whoi.edu/main/instruments/miso>). The Tow Cam system was equipped with a 16 megapixel still digital camera that transferred data from the camera and CTD in real time to the research vessel, which allowed a guided sampling effort. Additionally, we noted large-scale seafloor characteristics such as depressions, cracks, and rock slabs in the cruise log. Vertical CTD (SBE 9 plus sensor) profiles of seawater hydrography were taken at each location. Water collected from the CTD was used to measure water column methane concentrations. We also collected qualitative core samples in order to analyze sediment characteristics such as porosity, grain size, total organic carbon (TOC), benthic chlorophyll *a* (Chl *a*) pigments, and sediment methane concentrations.

Table 1. Summary information for sampling and survey locations. Station locations and names, date sampled, gear used, station abbreviations and core #, coordinates, and depth.

Location	Date	Sampling gear	Station	Latitude °N	Longitude °E	Depth (m)
VR1 active seep	28 Jun 2014	Multicore	VR1 #676	79° 00.5	06° 54.2	1207
	20 May 2015*	Tow Cam	VR1 #888			
VR2 active seep	20 May 2015	Tow Cam	VR2 #891	79° 00.4	06° 53.9	1204
VR3 active seep	20 May 2015	Tow Cam	VR3 #896	79° 00.2	06° 55.4	1203
SvR inactive	23 Jun 2014	Box core	SvR1 #656	78° 18.2	05° 48.0	1577
SvR inactive	23 Jun 2014	Multicore	SvR2 #658	78° 21.3	05° 47.1	1614
SvR inactive	23 Jun 2014	Multicore	SvR3 #659	78° 30.2	05° 42.7	1706

*Date of sampling, qualitative characteristics.

Infaunal samples

In total, we sampled 20 quantitative core samples, nine from the active VR (three stations) and 11 from the inactive SvR (three stations) in order to characterize macro-infaunal communities. In this survey, we have targeted macrofauna ($\geq 500 \mu\text{m}$) that live mainly inside the sediment and are hereafter referred to as “infauna.” The samples were sieved on board with a mesh size of $500 \mu\text{m}$. Material retained on the sieve was fixed in formaldehyde (4%), mixed with rosebengal for staining living tissues, and the solution was buffered with borax (sodium tetra-borate decahydrate). Samples were sorted and identified to the lowest possible taxon and stored in 80% ethanol. This procedure followed the ISO 16665:2014 fieldwork protocols to ensure consistency and quality control of benthic faunal surveys. Organisms were first separated into five main phyletic groups: Crustacea, Echinodermata, Mollusca, Polychaeta, and Diverse (containing members of Brachiopoda, Nemertea, Oligochaeta, and Sipuncula). Each individual was counted and weighed (aggregated wet weight in phyletic groups). Planktonic taxa were excluded from analysis as were Foraminifera and Nematoda since such taxa are not properly retained on a $500 \mu\text{m}$ mesh size.

Megafaunal communities and seafloor images at Vestnesa pockmarks

In order to characterize epifaunal megafauna from VR, we took a continuous series of seafloor images every 15 s along two transects from the outside of the active pockmarks moving toward the center of the feature. Images were taken at an altitude of approximately 2.5–5 m above the seafloor and were analyzed for the distribution and abundance of megafauna. We assigned images into three spatial categories (hereafter referred to as “locations”) relative to the center of the pockmark: “Outside,” “Edge,” and “Inside.” These designations were determined based on habitat changes observed from the images in relation to ship/camera location at the pockmark. A total of 144 images were analyzed from two transects that moved progressively from the outside to the inside of the two pockmarks (one transect at each pockmark;

Fig. 2). Each image was manually analyzed, and the presence or absence of visible epifaunal megafauna taxa was noted (hereafter visible epifaunal megafauna is referred to as “megafauna”). The resolution of seafloor images did not always allow identification of taxa to species-level. Instead, taxa were grouped into morphologically different faunal groups based on higher taxonomical ranks (i.e., phylum, class, and order), appearance, and size.

Methane measurements in sediment and water column

For compositional analyses of methane in water and sediments at each region (VR and SvR), a conventional headspace sampling preparation technique was applied. Bulk sediments (5 mL), collected from sediment cores, were subsampled with a plastic syringe. The sediments were transferred into 20 mL headspace glass vials containing 5 mL of 1-molar NaOH solution and two glass beads. Vials were immediately capped with rubber septa, sealed with aluminum crimp caps and shaken. Seawater was collected with 5 L Niskin bottles mounted on a 12-bottle rosette for water column vertical profiling. Immediately after recovery of the rosette, 60 mL plastic syringes were flushed three times and filled with water aliquots from Niskin bottles. Five milliliters of pure nitrogen gas was introduced into each bottle as a conventional headspace and the syringe was shaken for 2 min to allow the headspace nitrogen to equilibrate with the dissolved methane in the water sample. Sediment and water samples were stored at 2°C prior to analysis, and were analyzed within 1–2 h.

Methane and other hydrocarbon concentrations were determined with a gas chromatograph (GC) ThermoScientific FOCUS GC equipped with a flame ionization detector (FID). Only methane was separated in water samples at 170°C and with the isothermal oven temperature set to 40°C. To separate methane and other hydrocarbons in sediment samples, temperature was altered between 40°C, 70°C, and 120°C. Hydrocarbon gases were separated on a column RESTEK HS-Q 80/100, 2 mm using hydrogen as the carrier gas. The system was calibrated with external standards of 2 ppm and 30 ppm (Air Liquide).

Table 2. Grain size (fraction of pelite < 63 μm) and TOC (%) from upper 30 cm multicore samples at VR (active seep) and SvR (inactive control). Numbers in bold indicate highest recorded number. Group means presented at the bottom of the table (\pm SE).

Interval	Vestnesa		Svyatogor	
	Pelite	TOC	Pelite	TOC
0–1 cm	54.6	0.53	62.5	0.68
1–2 cm	66.3	1.01	82.1	0.89
2–4 cm	72.0	1.58	81.5	1.69
4–6 cm	76.4	1.71	79.8	1.22
6–8 cm	87.5	1.82	76.2	0.96
8–10 cm	79.8	1.56	79.8	1.04
10–12 cm	90.3	1.67	72.4	0.94
14–16 cm	85.8	1.60	79.6	0.64
18–20 cm	87.5	1.39	87.2	0.72
25–30 cm	82.5	1.28	94.5	1.59
Mean \pm SE	78.3 (3.6)	1.42 (0.12)	79.6 (2.7)	1.04 (0.12)

For methane concentrations in sediments, porosity data from benthic sediment sampling was used to convert gas chromatograph (GC)-flame ionization detector (FID) results between ppm and nmol. Methane concentrations in water samples presented here in nmol L⁻¹ were calculated according to Wiesenburg and Guinasso (1979) with consideration of salinity, sample temperature, and ambient atmospheric pressure.

Benthic pigment and sediment analysis

Sediment samples were collected to measure benthic Chl *a* and phaeopigments (PhP), as indicators of photosynthetically based organic material at the two regions, VR (active) and SvR (inactive). Sediment Chl *a* indicates the fresher, relatively recently produced material settled at the seafloor, whereas PhP are a degradation product of Chl *a*. Sediment pigment concentrations from the two regions (VR and SvR) were analyzed by fluorometry in accordance with Holm-Hansen et al. (1965). Chl *a* and PhP samples were extracted with acetone for 24 h in the dark, centrifuged, decanted, and measured for fluorescence in a Turner Design Model 10 AU fluorometer before and after acidification with hydrogen chloride (HCl). The measured concentrations were corrected for sediment porosity.

Porosity of sediment samples from both regions was determined by using a wet-dry method where pre-weighed vials of known volume were filled with sediment, reweighed and later dried at 60°C until all water evaporated (Zaborska et al. 2008). The density of the sediment was calculated by using the basis from the wet weight of sediment and water combined.

Sediment grain size (fraction of pelite < 0.63 μm) and TOC were determined by subsampling core samples (minimum 50 g) from downcore profiles from the two regions.

Grain size was determined according to Bale and Kenny (2005). The TOC samples were analyzed with a Shimadzu SSM TOC 5000 and Elementar Vario TOC Cube.

Statistical analysis

Infaunal data

Infaunal abundances from core samples were used to calculate community diversity parameters including species richness (*S*), Evenness (*J'*), Shannon Wiener Diversity (*H'* log_e). Single square-root transformation and standardization were carried out on infaunal abundances to balance the impact of both highly abundant and rare taxa in the same dataset. Abundance data was also used to conduct a principal component analysis (PCA) (non-parametric test, Primer[®] 6; Clarke and Gorley 2006). To test differences in community structure and biomass, an analysis of variance (ANOVA) (non-parametric single-factor ANOVA: Kruskal-Wallis test on ranks) was used, with “methane seepage” (i.e., active vs. inactive) as the dependent variable. All pairwise comparisons were made using Dunn’s test with an overall significance level of $p \leq 0.05$ using SigmaPlot v.12.5.

Megafaunal composition

The presence/absence data of faunal groups from the seabed photos were analyzed with a two-factor ANOVA (dependent variables “pockmark” and “location”) to detect differences between the two pockmarks (Lunde and Lomvi) and among the three assigned locations (“Outside,” “Edge,” “Inside”). Analysis by two-factor ANOVA, after testing the conformity of the dataset for the assumptions of ANOVA (normality of distributions and homogeneity of variances) was performed on square-root transformed data using SigmaPlot v12.5.

Species richness data from presence/absence of taxa was assembled in Primer[®] 6, in a Bray-Curtis similarity matrix based on the number of taxa represented at each image. This was followed by a two-way similarity percentage analysis (SIMPER) in order to identify the dissimilarity in species richness between the groups based on “location” and “pockmark” and a PCA in order to identify the faunal taxa contributing most to the variance of each group (i.e., “location” and “pockmark”).

Environmental statistical data—sediment and methane

We used various statistical tests to differentiate environmental and sediment characteristics of the two regions; active VR and inactive SvR. Downcore profiles (0–30 cm, 10 samples) of sediment grain size (% pelite) and TOC satisfied the conditions of normality and equal variance and were tested with a Student’s *t*-test to identify significant differences between VR and SvR. Sediment Chl *a* and benthic pigment concentrations between VR and SvR were compared with a single-factor ANOVA after the data were examined for normality and equal variances. The power of the tests was below the desired < 0.8 due to small sample size per

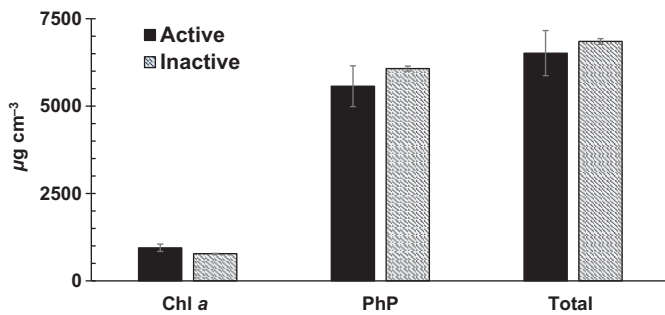


Fig. 3. Mean sedimentary pigment concentration, Chl *a*, and PhP, from upper sediment (0–2 cm) at Vestnesa (active) and Svyatogor (inactive). Error bars indicate \pm SE.

treatment. Downcore methane measurements (ppm) from both VR and SvR were log-transformed to reduce the large variation among locations and samples and analyzed with a single-factor ANOVA (these data satisfied the condition of equal variance but not normality, $0.046 < 0.05$).

Results

Environmental characteristics

Both regions, active VR and inactive SvR, exhibit oceanographic characteristics of a typical Arctic deep-sea habitat located below 1200 m of water depth, possessing dense bottom water with high salinity (34.9 psu), sub-zero temperatures (-0.8°C), and relatively high oxygen content (5.4 mL L^{-1}).

Grain size, % pelite ($< 63 \mu\text{m}$), in the upper 30 cm of sediment (Table 2) did not show any significant differences between the regions, VR (mean 78.3 ± 3.6 SE) and SvR (mean 79.6 ± 2.7 SE), $t(18) = -0.290$, $p > 0.05$). Both regions exhibited a downcore increase in the pelite content. At active VR, the surface (0–1 cm) sediment pelite fraction was 54.6% compared to 62.5% at inactive SvR, while at 25–30 cm pelite concentrations were 82.5% and 94.5%, respectively. The TOC content of sediments was higher at VR compared to SvR stations ($1.42\% \pm 0.12$ SE vs. $1.04\% \pm 0.12$ SE), ($t(18) = 2.244$, $p < 0.05$) (Table 2).

Chl *a* and PhP concentrations in the upper 0–2 cm surface sediment from VR and SvR were not significantly different, $p > 0.05$, ($F(1,4) = 0.64$, $p = 0.47$), (Fig. 3). The ratio between the amount of fresh production (Chl *a*) and degraded pigments (PhP) was 17% at VR and 13% at SvR showing that VR had a slightly higher portion of “fresh,” recently produced Chl *a*.

The main environmental difference between the regions, active VR and inactive SvR, was the presence of methane. In the bottom water at VR, the methane concentration was 76.4 nmol L^{-1} , whereas at SvR the concentration was 2.2 nmol L^{-1} . Methane concentrations were significantly higher $p < 0.05$, ($F(1) = 232.6$, $p < 0.001$) in the sediment at VR compared to SvR. Downcore profiles of methane in the sediment at VR varied between 262.0 ppm at the sediment surface and

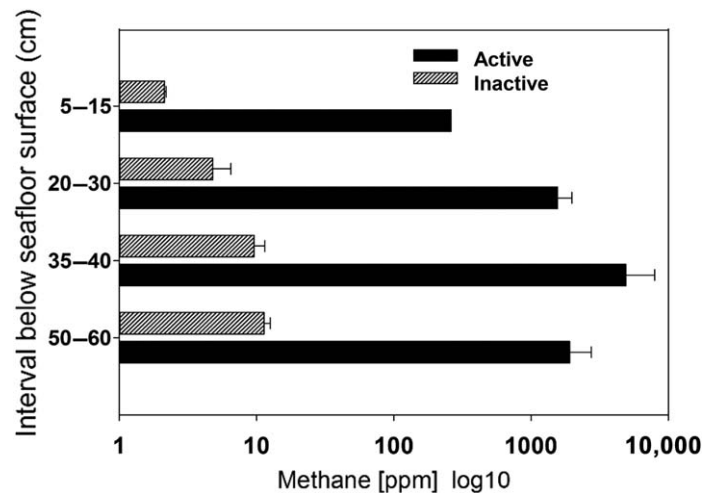


Fig. 4. Downcore sediment methane concentration [ppm] at Vestnesa (active) and Svyatogor (inactive), (interval mean values \pm SE).

1911.5 ppm at 60 cm below the seafloor (Fig. 4); with maximum value for an individual sample of 9219 ppm at 39 cm below seafloor level (bsfl). At SvR, the methane concentration in the sediment ranged from 2.1 ppm to 11.3 ppm from 0–60 cm bsfl, with a maximum sample value of 13.7 ppm at 54 cm bsfl. We recovered pieces of gas hydrate from sediments at VR collected from gravity cores.

Seabed features at Vestnesa pockmarks

Different habitats at VR are observed when moving along transects into the depression of the two active pockmarks Lunde and Lomvi. Inside these pockmarks, hard rock features, identified as carbonate outcrops compose reef-like 3D structures among scattered patches of soft-bottom sediment covered by microbial mats and worm tufts (chemosymbiotic siboglinid polychaetes) (Figs. 5, 6). Toward the edge of each pockmark, carbonate outcrops disappear, and soft-bottom sediments with patches of microbial mats and worm tufts predominate. Outside pockmarks, the seabed is dominated by relatively homogeneous and featureless deep-sea soft-bottom plains, interrupted by ice rafted-debris such as drop stones (Fig. 5).

Megafaunal patterns at active pockmarks

The large-scale structural habitat differences (see previous section) at the two pockmarks clearly influences the composition of megafauna (Figs. 6, 7) at the three main locations (“Outside,” “Edge,” “Inside”). “Inside” the pockmark, the community was composed of a combination of hard- and soft-bottom living organisms. Foliose and calcareous bryozoans, stalked hydroids, small gastropods, different species of sponges and large pycnogonids (possibly *Colossendeis* sp.) occurred on the carbonates (Fig. 5f), occasionally with gadi-form fishes (rockling-like morphotype). Between carbonate outcrops, soft-bottom patches were colonized by microbial mats and siboglinid worm tufts which were often associated

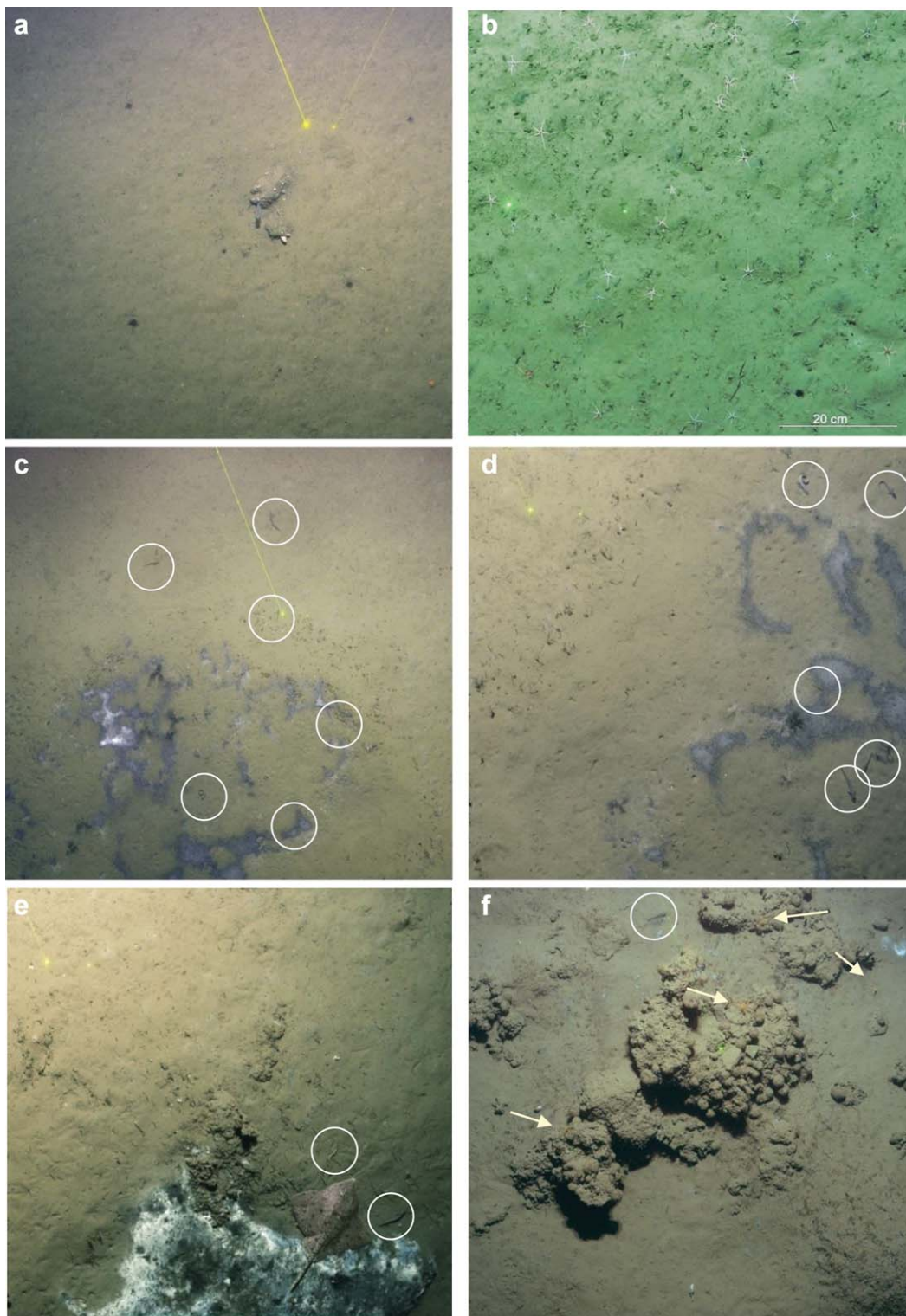


Fig. 5. The three main locations relative to pockmarks Lomvi and Lunde. Photos (a–b) show “Outside,” soft bottom locations with ice rafted drop stones, epifauna, soft-bottom anemones, and ophiuroids. Photos (c–d) show “Edge,” where microbial mats, black sediment patches, and siboglinid worm tufts occur together with aggregations of zoarcidae fishes. Photos (e–f) show “Inside” locations with large carbonate outcrops and various megafauna such as sponges, sea spiders and snails and also different species of zoarcidae fishes and a skate. Distance between green lasers dots is 20 cm. White circles indicate zoarcids, arrows point out pycnogonids.

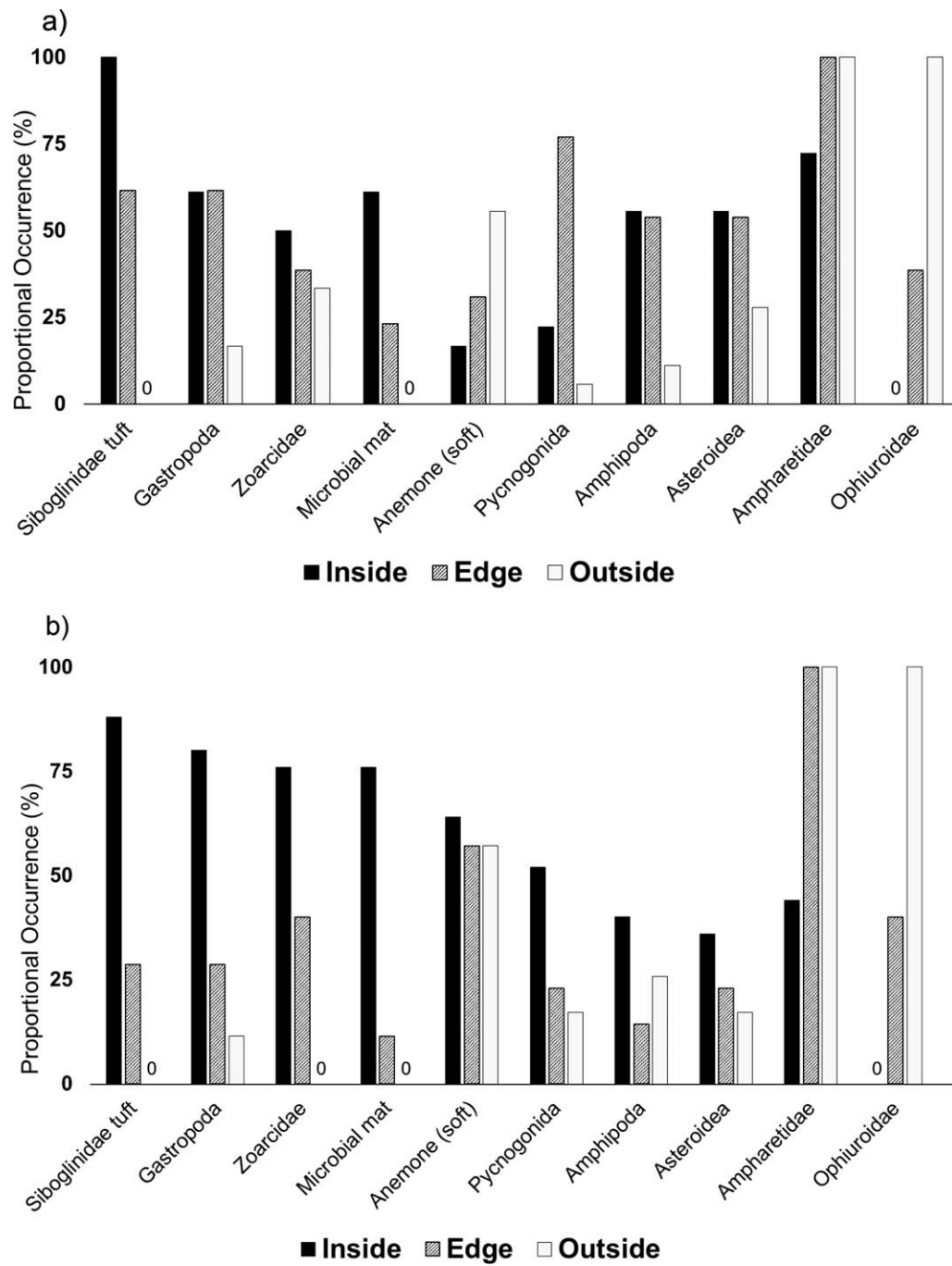


Fig. 6. Megafaunal species richness based on presence/absence in individual photos at each location. Upper (a) shows pockmark Lunde faunal composition and lower (b) shows Lomvi.

with different species of zoarcid fishes. Based on morphotypes and appearance, we suggest at least three different species of zoarcids are represented in the photos: (1) *Lycodes squamiventer* Jensen, 1904, (2) *Lycodonus flagellicauda* (Jensen, 1902), and (3) *Lycodes frigidus* Colett, 1879. They are all known at the VR region and recognized from Arctic waters (Bergmann et al. 2011; Meyer et al. 2013). Soft-bottom

anemones, ampharetid-like polychaetes (hereafter referred to as ampharetids), and large buccinoid gastropods (possible *Colus* sp.) are observed between carbonate outcrops. We also occasionally observe skates, similar to *Amblyraja hyperborea*, (Collett, 1879) (Figs. 5e, 8) and pale-whitish starfish (Asteroidea, possibly *Bathybiaster* sp.). Carbonate outcrops disappear toward the “Edge” location, however, microbial mats and

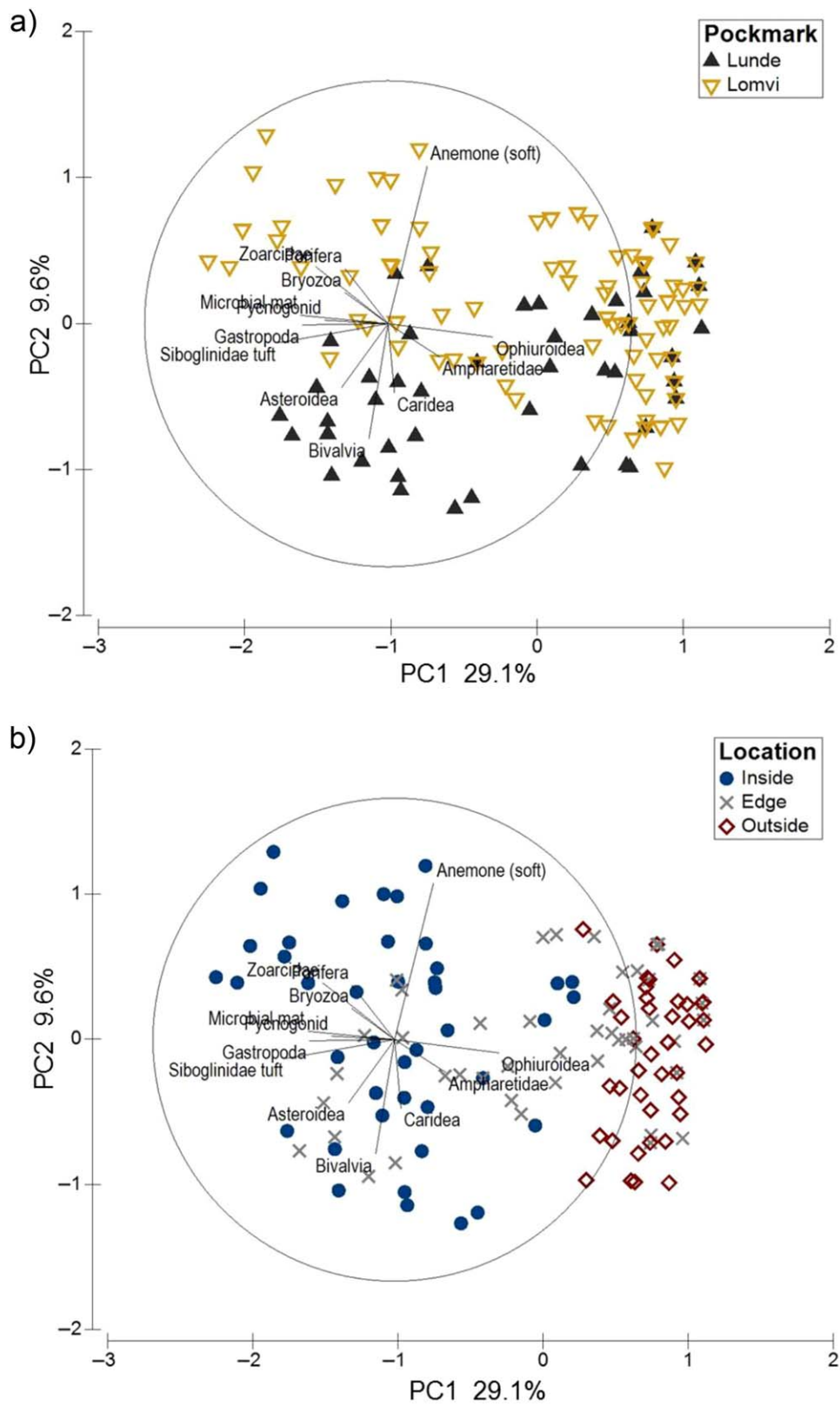


Fig. 7. PCA on presence/absence of megafaunal taxa identified from a total of 144 images at pockmarks Lomvi and Lunde. **(a)** Individual photo-replicate coded for “Pockmark” (Lomvi, Lunde). Taxon names are displayed for faunal groups where at least 20% of the variance is explained on the first two PC-axes. **(b)** Individual photo-replicate coded for factor “Location” (Inside, Edge Outside). [Color figure can be viewed at wileyonlinelibrary.com]



Fig. 8. A sea-spider and buccinoid gastropod in a “meadow” of siboglinid worms at the Lomvi pockmark. At the lower right, a skate is partly buried with sediments. Distance between laser points = 20 cm.

siboglinid tufts remain common (Fig. 5c,d) indicating a diffuse methane flux at this locality. The microbial mats and the siboglinid tufts present at the “Edge” are mixed with conventional deep-sea fauna including ampharetid polychaetes, anemones, pycnogonids, gastropods, and amphipods. Along the “Edge,” microbial patches and siboglinid tufts gradually disappear and the seafloor becomes densely populated by ophiuroids. Outside the pockmark, at the expansive soft-bottom plains, ampharetids and ophiuroids are the predominant visible megafaunal taxa (Figs. 5b, 6). Other sporadically visible megafauna includes the deep-sea sea-pen *Umbellula encrinus*, Linnaeus, 1758, skates, soft-bottom anemones, amphipods, bivalves, and starfish. The mean density of ophiuroids outside both pockmarks is 49 ± 3.5 (SE) ind. m^{-2} , (54 ± 4.5 ind. m^{-2} in the proximity of pockmark Lomvi compared to 44 ± 5.0 ind. m^{-2} at Lunde: single *t*-test, $t(18) = -1.542$; $p > 0.05$).

A two-way ANOVA tested the factors “pockmark” (Lunde or Lomvi) vs. “location” (Inside, Edge, Outside) for megafaunal composition. We found significant differences between pockmarks ($p < 0.001$) and among locations ($p < 0.001$) (Table 3). “Inside” megafaunal species richness was significantly higher than “Outside” at both pockmarks, however, pockmark Lunde had significantly higher overall taxon richness compared to Lomvi. The “Edge” locations differed between the two pockmarks and was significantly different from each other in terms of faunal composition (Fig. 6). The faunal community at location “Edge” was either similar to the “Outside” community (for Lomvi) or more similar to the “Inside” community (Lunde). This pattern explains the significant interaction term in the ANOVA (Table 3).

Table 3. Results of two-way ANOVA of megafaunal presence/absence species richness from photo transects for the factors “pockmark” and “location.”

Factors	df	SS	MS	F	p
Pockmark	1	1.924	1.924	16.185	<0.001
Location	2	7.595	3.798	31.95	<0.001
Pockmark × location	2	3.324	1.662	13.983	<0.001
Residual	138	16.404	0.119	—	—
Total	143	30.298	0.212	—	—

Abbreviations: df: degrees of freedom, SS: sum of squares and MS: mean square

The SIMPER analysis of presence/absence of megafaunal taxa identified from the seafloor images demonstrate that average dissimilarity between pockmark “Lomvi” and “Lunde” across all locations (Inside, Edge, Outside) was 49.6%, where “Anemone” (soft) and “Bivalvia” represented the largest dissimilarities. This separation between the two pockmarks is observed in the PCA-plot of the presence/absence of identified megafauna and where “Lunde” and “Lomvi” are separated along the y -axis, PC2 (Fig. 7a). Between locations for both pockmarks, the highest average dissimilarity is seen for locations “Inside” and “Outside” (75.4%) and the largest differences is recorded for the faunal taxa “Ophiuroidea” and “Siboglinidae,” comprising a dissimilarity of 12.2% and 11.1%, respectively. These differences between “Outside” and “Inside” locations are indicated in the PCA (Fig. 7b) where the taxa “Ophiuroidea” and “Siboglinidae” are split along the x -axis (PC1).

Infaunal community structure

There are clear differences in infaunal composition and community structure between the active VR and inactive SvR regions. There is no overlap among the top five most dominant taxa at VR stations compared to those at SvR (Table 4). For the entire survey (active and inactive samples combined), the top five most dominant taxa contributed to 61.6% of total infaunal composition: for VR, they contributed to 70.1% and for SvR the contribution is 75.4%. The PCA (Fig. 9) illustrates the separation between active and inactive stations and replicates with infaunal taxa clearly separated along the x -axis (PC1), distinguishing active seep samples from inactive controls. Among individual replicates (Fig. 9), the SvR samples are more dispersed along the y -axis (PC2) compared to VR replicates. This indicates a larger faunal variation among samples at the inactive SvR relative to the active VR samples.

Total infaunal abundance tested in a one-way ANOVA for the factor “methane seepage” shows a significant difference ($p \leq 0.05$) between the VR and SvR samples (Table 5). Aggregated total faunal abundance (group mean of all stations, separated by location, i.e., active VR or inactive SvR) is more

Table 4. Top five most common taxa (in bold) in relative percentage and density (0.1 m⁻²) based on faunal abundances in the total survey and separated by region (active VR and inactive SvR). The number of total samples is listed in parentheses below each location. Faunal group abbreviations in parentheses. Biv, Bivalve; C, Crustacea; O, Oligochaeta; Pol, Polychaetes; P, Priapulida; S, Sipuncula.

Taxa	Total (20) (%)	Density ind. 0.1 m ⁻² (± SE)	Active (9) (%)	Density ind. 0.1 m ⁻² (± SE)	Inactive (11) (%)	Density ind. 0.1 m ⁻² (± SE)
Tanaidacea indet. (C)	39.0	166 (164.2)	48.4	369 (364.5)	0.0	0
Cirrophorus branchiatus (Pol)	7.8	33 (10.5)	0.0	0	40.0	60 (14.7)
Siboglinidae. indet (Pol)	5.5	24 (15.1)	6.9	52 (31.9)	0.0	0
Oligochaeta indet (O)	4.9	21 (11.1)	6.1	47 (22.4)	0.0	0
Thyasira dunbari (Biv)	4.3	18 (6.6)	5.4	41 (10.6)	0.0	0
<i>Aricidea hartmani/Ophryotrocha sp. (Pol)</i>	2.7	25 (4.8)/11 (11.5)	3.3	25 (8.8)/25 (25.4)	0.0	0
<i>Golfingia sp. (P)</i>	3.6	15 (5.4)	0.6	4 (2.2)	16.2	24 (9.0)
Sipunculida indet (S)	1.8	8 (2.1)	0.2	1 (1.4)	8.5	13 (3.0)
<i>Myriochele heeri (Pol)</i>	1.2	5 (2.3)	0.0	0	6.2	9 (3.9)
<i>Praxillura logissima (Pol)</i>	1.2	5 (1.4)	0.4	3 (1.9)	4.6	7 (2.0)
Total sum top 5	61.5	—	70.1	—	75.5	—

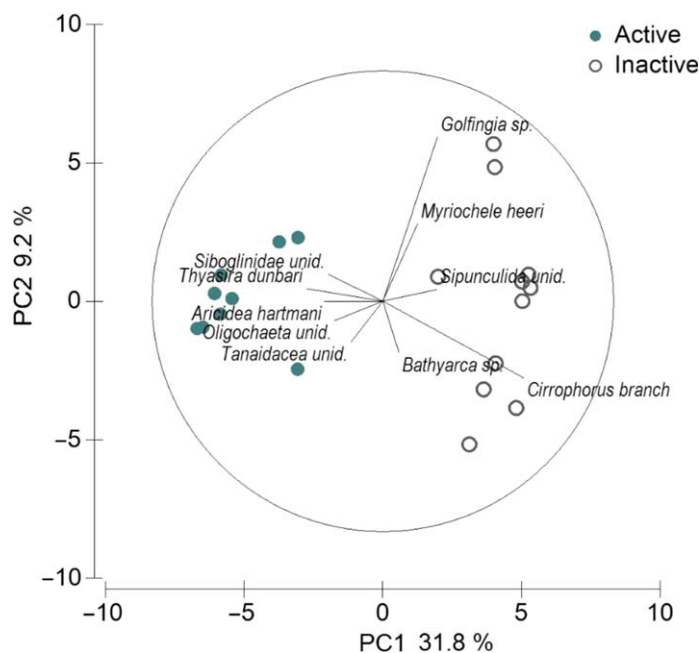


Fig. 9. PCA based on infaunal abundances from Vestnesa (active seep) and Svyatogor (inactive). Taxon names are displayed for faunal groups where at least 20% of the variance is explained on the first two PC-axes. There is a clear separation on PC1 (x-axis) between taxa found at the active VR stations compared to taxa recorded at the inactive SvR controls. [Color figure can be viewed at wileyonlinelibrary.com]

than five times higher at VR compared to SvR, mean 782 ± 380 (SE) ind. m⁻² and 150 ± 20 (SE) ind. m⁻², respectively (Fig. 10a).

The highest and lowest mean biomass per station is 5.07 g ww 0.1 m⁻² at Sta. VR1 and 0.47 g ww 0.1 m⁻² at Sta. SvR2, respectively (Table 6). Total infaunal biomass is

Table 5. Results of one-way non-parametric ANOVA (Kruskal-Wallis test) testing for differences in infaunal community parameters between the active Vestnesa and inactive Svyatogor regions. Median, percentiles (25% and 75%) and p-value are shown for the faunal parameters; “Abundance” 0.1 ind. m⁻², “Biomass” wet weigh grams 0.1 m⁻², “Species Richness,” “Diversity,” and “Species Evenness.”

	Group	Median	25%	75%	p
Abundance	Active	497	242	579	<0.001
	Inactive	140	115	204	—
Biomass	Active	2.97	1.30	3.88	<0.01
	Inactive	0.48	0.19	0.80	—
Species richness	Active	14	9	19	<0.001
	Inactive	6	5	7	—
Diversity (H')	Active	2.03	1.84	2.78	<0.01
	Inactive	1.47	1.33	1.60	—
Evenness (J')	Active	0.81	0.78	0.95	0.54
	Inactive	0.86	0.79	0.95	—

five times higher at VR compared to SvR (Fig. 10a). This difference between the two locations is significant (one-way ANOVA; p < 0.05) (Table 5). Species richness (S) and diversity (H') are significantly different between VR and SvR (one-way ANOVA; p < 0.05) (Table 5; Fig. 10b). Comparing species evenness (J'), the difference between active and inactive locations is not significant (one-way ANOVA; p > 0.05).

In the overall survey, encompassing 20 replicate cores, 74 taxa were identified, distributed among seven phyla. The phylum Annelida (class Polychaeta) contributes more than half of the 74 identified taxa (41) and represents 32.8% of the total relative faunal abundance. The second largest taxonomic group is Mollusca, divided among 13 taxa and

represented 10.9% of the overall total relative abundance. The single most relative abundant taxon, however, is small crustaceans in the order of Tanaidacea unid., contributing to

39.0% of the total relative faunal abundance (Table 4). The second largest relative abundant taxon is the polychaete *Cirrophorus branchiatus* Ehlers, 1908. This taxon is only present at inactive SvR stations. The chemo-associated family of polychaetes, Siboglinidae, is the third most common taxon in the entire survey, representing 5.5% of all organisms; it is only recorded at stations from VR. Tanaidacea (tanaids) is the most numerically dominant taxon in the survey because of a mass occurrence in one replicate; at Sta. VR3, the density is 3310 individuals 0.1 m^{-2} (density calculated from core samples). In total, tanaids are only recorded in four out of 20 samples, all from VR. Mean (\pm SE) infaunal densities in the overall survey is $433 \pm 168\text{ ind. }0.1\text{ m}^{-2}$ per station but with a large variation among individual core replicates ($64\text{--}3769\text{ ind. }0.1\text{ m}^{-2}$). The lowest grouped mean total abundance per station is $140\text{ ind. }0.1\text{ m}^{-2}$ (Sta. SvR2) and the highest abundance is $1235\text{ ind. }0.1\text{ m}^{-2}$ (Sta. VR3) (Table 6). Polychaetes dominate the total infaunal biomass, contributing more than 50% to total relative biomass, second largest is the group “Diverse,” contributing 17.5% to the total relative infaunal biomass in the overall survey.

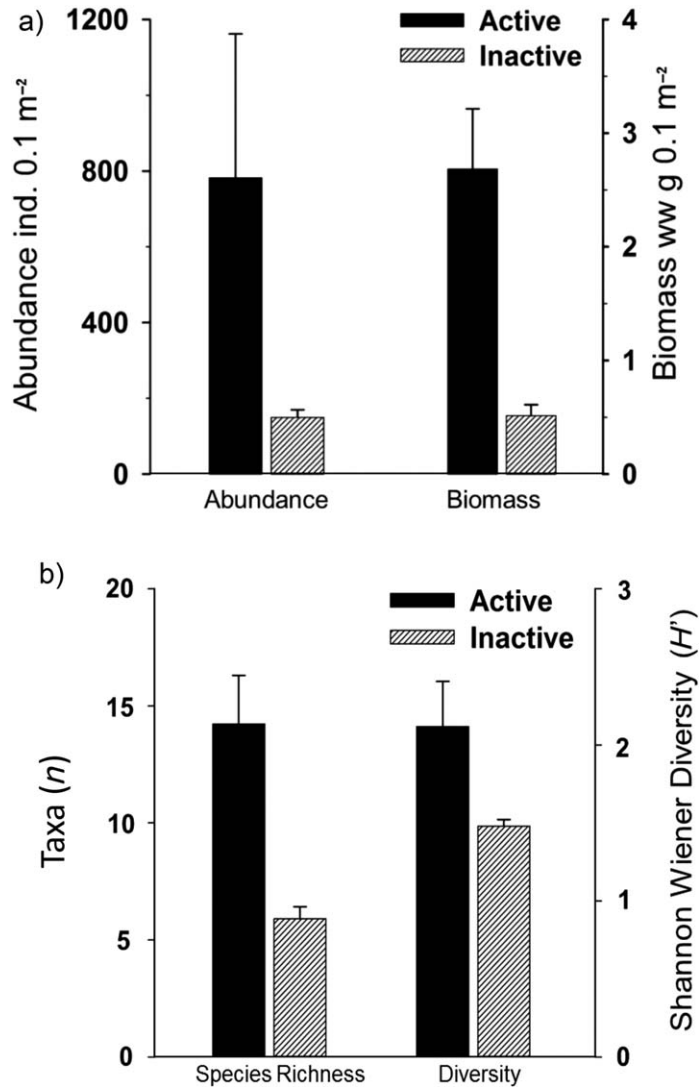


Fig. 10. Infaunal community parameters at active VR and inactive SvR sites. (a) Mean infaunal abundance and biomass, and (b) mean species richness and Shannon Wiener diversity (H'). Faunal parameters were all significantly higher ($p < 0.05$) at VR. Error bars indicate \pm SE.

Discussion

Methane—an energy source for benthos at VR

VR and SvR are two high-Arctic regions located at water depths greater than 1200 m. Both VR and SvR exhibit deep-sea characteristics (Sanders and Hessler 1969) regulated by sub-zero temperatures and high-Arctic seasonal variations. There were no differences in water temperature, salinity, oxygen concentration, grain size, or sedimentary pigment concentration (photosynthetically produced organic matter) between VR and SvR. The main extrinsic difference between these two regions is methane seepage. We recorded sediment concentrations of methane up to 100–1000 times higher in upper surface sediment layers (0–60 cm bsfl) and 50–70 times higher in bottom water at VR compared to SvR (Fig. 4). Bottom water methane concentration at SvR (2.2 nmol L^{-1}) is considered background concentrations for marine environments (Rehder et al. 1999; Gentz et al. 2014).

Marine environments in the Arctic are characterized by strong seasonality with respect to input of photosynthetically derived organic matter during a short and intense productivity

Table 6. Infaunal parameters from individual stations at VR and SvR: Species richness, density (individuals 0.1 m^{-2}), biomass (wet weight g 0.1 m^{-2}), Shannon-Wiener diversity, and Species Evenness.

Station	Species richness	Density (ind. 0.1 m^{-2})	Biomass (ww g 0.1 m^{-2})	H'	J'
VR1	15	573	5.07	1.90	0.70
VR2	41	382	2.41	2.52	0.92
VR3	30	1235	2.36	1.88	0.74
SvR1	17	149	0.51	1.50	0.84
SvR2	10	166	0.47	1.32	0.87
SvR3	9	140	0.59	1.65	0.88

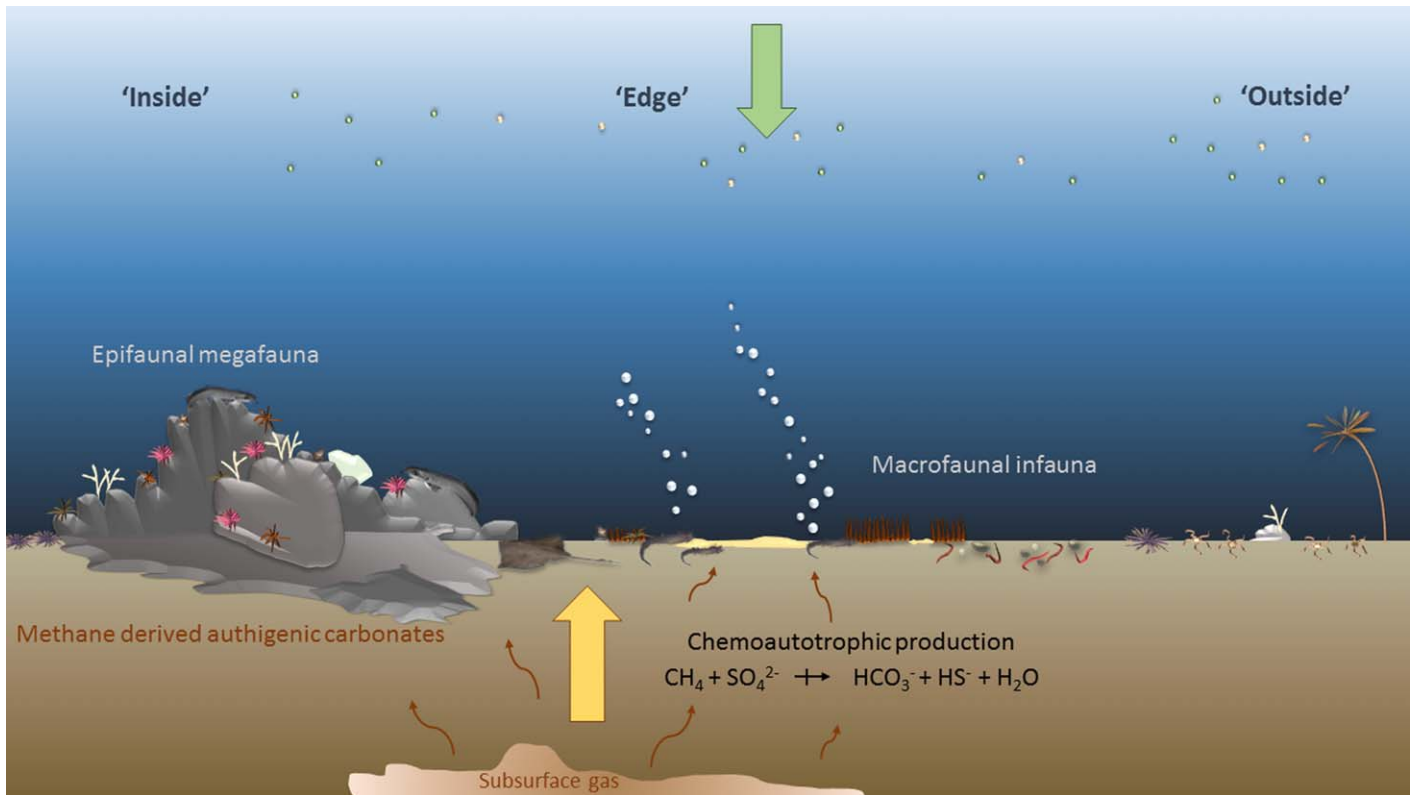


Fig. 11. Schematic representation of the key habitat structures and processes occurring at the high-Arctic cold seep oasis at VR. An autochthonous (local) chemosynthetic energy source (yellow arrow) in addition to the photosynthetically derived detrital matter (green arrow) from the water column, in combination with hard substrate provided by the carbonate outcrops enhances both communities of infaunal macrofauna and epifaunal aggregation of megafauna at this site.

season (Sakshaug 2004; Søreide et al. 2006; Ardyna et al. 2013). Photosynthetically derived organic matter produced in the photic zone and transported to the seafloor via trophic interactions and organic matter sedimentation is the energy source for conventional deep-sea ecosystems (Sanders and Hessler 1969; Rice et al. 1985; Gooday et al. 1990). The short productive season and the long transit of organic matter through the mesopelagic zone can result in high-Arctic deep-sea environments being food-limited over extended periods (Graf 1989). Compounds such as methane and sulfide, through microbial processes, can serve as an alternative local energy source for organisms that are able to utilize chemoautotrophic production in addition to photosynthetically-derived organics from the euphotic zone (Carney 1994). The similarity in all measured environmental parameters at active VR and inactive SvR, with the exception of methane, strongly suggests that methane emissions provide an alternative food source for conventional heterotrophic consumers at the deep VR seeps. Methane emissions result in a heterogeneous environment comprised of microbial mats, chemosynthetic worm tufts, and carbonate outcrops, providing 3D-structure and hard substrate at an otherwise relatively featureless and homogenous soft-bottom seafloor (Fig. 11).

Distinct infaunal taxa at methane enriched environments

There is little overlap in infaunal community composition between active VR and inactive SvR (Fig. 9; Table 4). None of the top five taxa from VR stations occurs at any of the SvR stations and the top five most abundant taxa from SvR are a minor part of the total relative abundance at VR. We attribute these differences to the methane activity at the cold seep. Four of the top five infaunal taxa at VR seeps (Table 4) are recognized from reduced environments including cold seeps (Dubilier et al. 2008; Blazewicz-Paszkowycz and Bamber 2011; Decker and Olu 2012). The most numerically dominant taxa among these is Tanaidacea that occurred en masse at Sta. VR3. Tanaid crustaceans are commonly observed in deep-sea macrobenthos (Bluhm et al. 2011) and have previously been identified at deeper shelf systems around Svalbard (Włodarska-Kowalczyk et al. 2004; Soltwedel et al. 2015) and cold seep environments along the Norwegian shelf (Blazewicz-Paszkowycz and Bamber 2011; Decker and Olu 2012). Tanaidacea can exploit both chemo-, and photo-autotrophic energy sources and have been suggested to feed on microbial mats, (Sellanes et al. 2011; Levin et al. 2016), which offer alternative food resources during periods of low organic matter input. The high densities of tanaids seen at VR are

comparable to densities of tanaids recorded both in cold seep habitats along the Norwegian shelf and from New Zealand. At the HMMV, tanaid densities near 20,000 ind. m^{-2} were recorded (Decker et al. 2012) in chemosymbiotic siboglinid fields of *Oligobrachia haakonmosbiensis* Smirnov, 2000, (also referred to as *O. webbi* in Meunier et al. 2010). Similarly, at Nyegga pockmark at the Norwegian shelf, 64° N, Decker et al. (2012) documented high occurrences of tanaids in fields of *Sclerolinum* cf. *contortum* Smirnov, 2000. High densities of Tanaids are also found at Svalbard shelf seeps (Åström et al. 2016). Presumably, the high densities of tanaids from the VR cold seep in this survey exemplifies the benefits of exploiting alternative food resources in deep-sea environments.

Oligochaetes are also taxa recognized from chemosynthetic habitats where some species (gutless oligochaetes) rely on microbial endosymbionts for nutrition (Blazejak et al. 2005; Dubilier et al. 2008). While we observed oligochaetes from several VR replicates, they were not present at SvR, and we can only speculate whether these oligochaetes rely on symbiosis with microbes for nutrition. The most abundant mollusk at VR is *Thyasira dunbari* Lubinsky, 1976, a high-Arctic species recorded from a wide range of circumpolar-Arctic habitats from both shallow bays and the deep sea. Thyasirids are a family of bivalves commonly known from reduced habitats, although they are not exclusively dependent on mutualistic trophic interactions with endosymbionts, and there is a wide range of nutritional dependence on symbionts within this family (Payne and Allen 1991; Dufour 2005; Taylor and Glover 2010). *T. dunbari* seems to be a highly adaptive species based on its habitat preferences. For example, Włodarska-Kowalczyk and Pearson (2004) documented high abundances of *T. dunbari* from a shallow, inner glacial bay community (< 100 m Kongsfjord, Svalbard) where the bay community was strongly influenced by glacial induced disturbance and high sedimentation rates. Furthermore, *T. dunbari* was the dominant macrofaunal species from deeper slopes > 1500 m in the Fram Strait representing over 20% of the total macrofaunal community (Soltwedel et al. 2015). The only obligate chemosynthetic infaunal taxa found in the present study is siboglinid worms, a chemo-obligate group of polychaetes that hosts microbial endosymbionts known to utilize methane and sulfur sources (Pleijel et al. 2009). We document high densities of siboglinid worms (2930 ind. m^{-2}) from one station at Vestnesa (VR1). Underwater photographs (Figs. 5, 8) reveal large, dense fields of siboglinid worms adjacent to seepage features including carbonate crusts and microbial mats inside the pockmarks. Due to difficulties in the taxonomy of this group and poorly preserved samples, identification to species level has not yet been possible.

In our survey, we see a number of taxa at active VR seeps that are directly (Siboglinidae) or partially dependent on or related to chemoautotrophy (Tanaidacea, Oligochaeta,

Thyasiridae) while these species are absent at inactive SvR. We also document higher TOC contents in sediments at VR compared to SvR (Table 2) with no differences in sedimentary pigment concentrations. This indicates that there is an additional source of organic carbon at VR that we suggest originates from chemoautotrophy. Hence, the influence of chemosynthesis on the infaunal community at VR is a viable explanation for the large observed regional differences in abundance, biomass, and diversity between the inactive SvR and active VR.

Enhanced infaunal community structure at methane enriched environments

There were large significant differences in infaunal community indices between the active VR and inactive SvR stations, with total abundance and biomass approximately five times higher at VR compared to SvR (Fig. 10a). The number of taxa (species richness) and Shannon Wiener diversity were also significantly higher at VR compared to SvR (Fig. 10b). The total infaunal abundance from all three VR stations (mean 782 ind. $0.1 m^{-2}$, Fig. 10a) is substantially higher than those reported from other macrobenthic studies in the region. Włodarska-Kowalczyk et al. (2004) documented average densities of 194 ind. $0.1 m^{-2}$ from “slope” Fram Strait, 79° N (500–1500 m deep) and Krönke (1998) reported densities of 120 ind. $0.1 m^{-2}$ from the Yermak Plateau, 80° N (> 800 m) and up to 155 ind. $0.1 m^{-2}$ from the Morris Jesup Rise 85° N (~ 1000–1600 m). Such densities are within the range of those recorded at the inactive SvR stations (mean 150 ind. $0.1 m^{-2}$), demonstrating that VR has an elevated overall total faunal abundance. Deep-sea environments are usually recognized as systems with low biomass, although the number of species and faunal diversity can be high (Sanders and Hessler 1969; Rex 1981). Cold seeps generally represent habitats of high species abundance and high biomass (Vanreusel et al. 2009; Cordes et al. 2010). High biomass has also been reported from cold seeps at the Svalbard shelf (Åström et al. 2016). The average biomass from VR stations (2.68 g ww $0.1 m^{-2}$) is slightly higher than the biomass recorded by Włodarska-Kowalczyk et al. (2004) at 1500 m in Fram Strait, where they reported much higher values compared to previous studies over the deep-sea Arctic basins (Paul and Menzies 1974; Krönke 1998). The total biomass from seep Sta. VR1 (Table 6) is similar in magnitude to troughs and depressions around the Svalbard shelf (< 500 m deep) (Carroll et al. 2008; Cochrane et al. 2012; Åström et al. 2016) and > 10 times higher than the shallowest stations along a latitudinal transect in Fram Strait ~ 2300 m (Vedennin et al. 2016). This indicates that infaunal biomass at our active deep-sea seep is comparable to adjacent shelf stations in Svalbard, and therefore suggests a substantial enhancement to the infaunal community from a localized energy source.

Species richness is, on average, over 2.5 times higher at the VR stations compared to SvR and Shannon Wiener diversity is also significantly higher at VR relative to SvR (Fig. 10b). The diversity indices from VR are, however, not unique in relation to similar studies, either from conventional deep-sea environments, or shallower shelf or fjords in Svalbard (Włodarska-Kowalczyk et al. 2004, 2012; Renaud et al. 2007; Vedenin et al. 2016). Cold seep systems or other chemosynthetic environments exhibiting strong chemical gradients are usually known to have high faunal abundance and high biomass but low diversity due to chemical stress from compounds such as hydrogen sulfide (Vismann 1991; Warwick and Clarke 1995; Bernardino et al. 2012). We observed the opposite, with the infaunal community at the VR active seep being more diverse than the non-seep control location. This could be a result of higher productivity via chemoautotrophy at the seep or due to an effect of deep-sea heterogeneity, where the SvR stations are comparatively barren, homogeneous, and food-limited. Species evenness is the only faunal index that did not show significant differences between active and inactive locations. In general, evenness is uniformly high in all stations, ranging from 0.70 to 0.98 with the exception of a single replicate with mass occurrence of tanaids ($J' = 0.26$). The species evenness values from our study are slightly higher than was documented from Svalbard shelf seeps (Åström et al. 2016). The relatively high J' in this survey may be related to the patchy distribution of organic matter in deep-sea environments (Rex 1981; Gage and Tyler 1991) and the relatively small abundance per sample of many different taxa.

Methane derived carbonate outcrops—a substrate for megafauna

The environment inside and outside pockmarks can vary substantially due to strong gradients in physical and environmental drivers such as currents, sedimentation, substrate and geochemistry, structuring faunal communities (Dando et al. 1991; Hammer et al. 2009; Webb et al. 2009a). Pockmarks from shallow shelves and slopes worldwide are known to attract aggregations of motile megafauna regardless of seepage activity, where local heterogeneity attracts “background” (conventional) fauna even when there is no gas seepage (Hovland and Judd 1988; MacDonald et al. 2010; Zeppilli et al. 2012). Regardless of depth and seep activity, pockmarks can also act as a refuge for slow growing species such as corals, cnidarians, and sponges as well as for fish populations especially in regions impacted by intense trawling pressure (Webb et al. 2009b; MacDonald et al. 2010; Clark et al. 2016).

There is a paucity of information on the ecology of deep-sea pockmarks (deeper than 1000 m), particularly, the association of seep communities and local, conventional fauna (Olu et al. 2009; Ritt et al. 2011). Our analysis of seafloor images reveals large changes in megafaunal composition along transects from outside and into the pockmarks. A key

driver of this faunal change is bottom substrate. Outside the pockmark, the environment is relatively homogenous, dominated by vast expanses of soft-bottom substrate. This outer locality (“Outside”) of the pockmarks shows a megafaunal pattern with an even distribution of ampharetids and brittle stars occasionally interrupted by the presence of soft-bottom anemones and motile organisms such as starfish, skates, bivalves, and amphipods. Burrowing tracks (or “lebensspuren”) in the sediment were commonly seen on the images, indicating activity of motile megafauna. This activity also creates micro-scale heterogeneity in the soft bottom environment (Quéric and Soltwedel 2007; Taylor et al. 2016). Epifaunal overgrowth and various fishes were commonly associated with drop stones on the surface seafloor, highlighting the importance of 3D structures and hard substrate on deep-sea soft bottom plains (Schulz et al. 2010; Meyer et al. 2014). The densities of ophiuroids recorded outside the VR pockmarks in this study (mean 49 ind. m^{-2}) are higher than those reported by Soltwedel et al. (2009) from nearby locations in Fram Strait (mean 16.7 ind. m^{-2}). Likewise, Meyer et al. (2013) reported similar densities (mean 16.5–19.2 ind. m^{-2}) of ophiuroids as Soltwedel et al. (2009) at 79° N, ~ 1200 m in Fram Strait in the first 2 yr of an inter-annual study of megabenthos; whereas during the last year, the density was significantly higher, (mean 49.6 ind. m^{-2}), and comparable to densities in this study. Generally, echinoderms are the dominant megafauna in the Arctic (Bluhm et al. 2011; Piepenburg et al. 2011) and brittle stars are considered to be the most prominent megafaunal group in Svalbard waters (Piepenburg and Schmid 1996; Piepenburg et al. 1996). Furthermore, it has been reported that the background community at HMMV, outside the caldera, is dominated by ophiuroids, mainly *Ophiocten gracilis* (Sars G.O., 1871) and *Ophiopleura borealis*, Danielssen and Koren, 1877 (Gebruk et al. 2003). In our study, there is not a single record of ophiuroids inside the pockmarks in relation to the carbonate outcrops, microbial mats nor the siboglinid worm tufts. Moving along transects from the “Outside” locality where ophiuroids are dominant toward the “Edge,” brittle stars gradually disappear and become completely absent in images where microbial mats and worm tufts appear. This observation could indicate that the brittle stars are sensitive to chemical compounds associated with the source location of the active seepage and thus only occupy habitats at the periphery of the pockmark. From Lau Basin in the Pacific Ocean, Sen et al. (2016) reported the presence of ophiuroids only from peripheral vent sites and attribute this to sulfide sensitivity since no detectable concentrations of hydrogen sulfide were recorded in the outer zones of the vents. Organisms occupying peripheral habitats may also benefit from increased productivity close to the seep because advection from seafloor emissions may influence the amount of particulate organic matter in adjacent areas. Increased vertical mixing can enhance water column productivity, supporting

nearby benthos and suspension feeders in the periphery of a seep or vent (Sorokin et al. 2003; Levin et al. 2016).

At the edge of the pockmark, the megafaunal composition changes, and all brittle stars are absent whereas siboglinid worm tufts and microbial mats become present. The overriding bottom type remains soft bottom with sporadic ice rafted drop stones and thus the main habitat difference at the “Edge” is the presence of microbial mats and tufts. Motile megafauna are frequently observed in association with tufts and mats, either adjacent to them or lying or sitting directly within them. This aggregation around specific biological seep features is mainly observed with sea spiders, zoarcids, snails, and amphipods within the “Edge” and the “Inside” locations. The “Edge” community is either similar to the “Outside” community or the “Inside” depending on the individual pockmark and its seafloor morphology and associated habitat gradients. This pattern is logical since photos were taken along a transect. We expect to find gradual changes in the habitat from both abiotic structures (carbonate crusts) and biotic structures (burrowing tracks and foundation organisms such as the siboglinids and microbial mats). At pockmark Lunde, there is a slightly higher mean species richness at the “Edge” megafaunal community compared to the community “Inside” (mean = 7.46 vs. 6.94) but this difference is not significant ($p > 0.05$). The phenomenon of higher species diversity at an edge-ecotype, however, is known as an “edge-effect” and implies that at the boundary of two shifting habitats there will be a mix of species from both habitats, possibly generating greater complexity and biodiversity (Livingston 1903; Harris 1988).

Large changes in habitat heterogeneity occur moving toward the “Inside” of the pockmark. Here, carbonate outcrops rise up to several meters above the surrounding seafloor. The “Inside” locality combines both hard and soft bottom substrates, allowing colonization by organisms with different habitat requirements or preferences. Correspondingly, we notice a large variety of visible megafauna (Fig. 6). We observed aggregations of zoarcid fishes primarily on or at the edges of microbial mats and worm tufts, lying on the seafloor in softer sediments between carbonate outcrops, whereas sea spiders and small gastropods were seen on top the carbonate outcrops. Various epifaunal taxa including sponges, hard-bottom anemones, bryozoans, and hydroids were attached to the carbonate structures. The occurrence of various organisms aggregating around reefs, outcrops, and other 3D structures is a well-known phenomenon from several studies comparing natural and artificial reef structures (Stone et al. 1979; Bohnsack 1989; Baine 2001). Habitat complexity, the physical substrate and shelter to avoid predation, are all believed to be important factors in attracting organisms to such structures (Stone et al. 1979; Wilson and Elliott 2009; Ashley et al. 2014). The physical difference between the soft bottom plains outside the pockmarks and the carbonate concretions inside is apparent and is reflected in the

megafaunal composition with significantly different taxon richness between the “Inside” and “Outside.” This pattern highlights the importance of such natural structures in an otherwise non-complex environment, namely, the deep-sea soft bottom plains.

The “oasis-effect” at active seeps

The pattern of megafauna at the methane seeping pockmarks is characterized by strong spatial differences in faunal composition and large aggregations of both low- and high-trophic level taxa. It is most likely related to two factors: (1) the reef-like MDAC provide a 3D structure and add complex heterogeneity to the deep sea, offering shelter and substrate to both sessile epifauna and motile fauna and (2) increased food availability from a local chemosynthetic source that supports a diverse community including aggregations of larger and higher trophic-level organisms (Fig. 11). These characteristics of the pockmark serve to attract organisms from the surrounding environment that interact with the chemosynthetic community.

Visual observations of the seafloor at VR indicate that methane emissions create seafloor heterogeneity unique to a cold seep system resulting in large habitat variability within the pockmark area. This heterogeneity, represented as a patchwork of microbial mats, worm tufts and the carbonate outcrops, likely drives the pattern of megafaunal species distribution along the transect. The presence of large, high-trophic level organisms around carbonate outcrops or drop stones exemplifies the importance of structural objects in deep-sea environments (Meyer et al. 2014). However, the presence of aggregated biomass and/or predatory organisms may also be related to food availability. Although we did not measure the isotopic composition ($\delta^{13}\text{C}$), indicative of overriding carbon source of organisms, there is little doubt that there is an additional source of nutrition supporting the infaunal community at Vestnesa seeps which is absent from the community at the SvR. Gebruk et al. (2003) reported highly depleted $\delta^{13}\text{C}$ of *Lycodes squamiventer* (-51.9‰) from a site at $76^{\circ}07' \text{N}$, $6^{\circ}10' \text{E}$, (referred to as VR in Gebruk et al. 2003 but located further south along Knipovich Ridge compared to sites investigated in this study), where they suggested that the diet of the zoarcids includes chemosymbiotic siboglinids (*Sclerolinum* sp.). Also, paleo-communities of chemosymbiotic vesicomyid bivalves ($\sim 17,000$ yr B.P.) from VR pockmarks exhibited depleted shell organic and inorganic $\delta^{13}\text{C}$, indicating partial nutritional dependency on chemoautotrophic production (Ambrose et al. 2015). We suggest that the infaunal community at VR is supported by chemoautotrophic production in the sediment in addition to the detrital energy derived via the conventional, photosynthetic carbon cycle. The enhanced community of infaunal organisms likely serves as a food source for larger megafauna aggregating around the carbonate structures. This hypothesis is also supported by the suggestion that siboglinid

polychaetes are included in the diet of zoarcids around seeps (Gebruk et al. 2003).

Summary

We have shown that active methane seepage strongly influences deep-sea benthos in the high-Arctic, resulting in enhanced infaunal abundance, diversity, and biomass compared to an inactive control region. We attribute these differences to the presence of methane and its utilization in the marine biosphere. Active hydrocarbon seepage and chemoautotrophic production at Vestnesa seeps influence benthos via mutualistic relationships and/or trophic interactions from microbes to megafauna. Thriving infaunal communities and habitat heterogeneity, both utilized by megafauna, produce a pronounced seep related “oasis effect” (Carney 1994; Levin et al. 2016). The Arctic deep seafloor oasis effect identified in this study may be the result of unique high-latitude environmental drivers such as strong seasonality and episodic productivity in the euphotic zone and sub-zero temperatures where seeps provide a refuge for conventional organisms compared to the relatively featureless, homogeneous, and food limited deep-sea surroundings.

Author Contribution Statement

Ideas and design of project: Åström, M. Carroll, J. Carroll, and Ambrose; Data collection: Åström, M. Carroll, Ambrose, and Silyakova; Data analysis and interpretation: Åström, Silyakova, M. Carroll, and Sen; Drafting the article: Åström; Revision of final version of the article: All authors.

References

- Ambrose, W. G., G. Panieri, A. Schneider, A. Plaza-Faverola, M. L. Carroll, E. K. L. Åström, W. L. Locke, and J. Carroll. 2015. Bivalve shell horizons in seafloor pockmarks of the last glacial-interglacial transition: A thousand years of methane emissions in the Arctic Ocean. *Geochem. Geophys. Geosyst.* **16**: 4108–4129. doi:10.1002/2015GC005980
- Ardyna, M., M. Babin, M. Gosselin, E. Devred, S. Bélanger, A. Matsuoka, and J.-É. Tremblay. 2013. Parameterization of vertical chlorophyll a in the Arctic Ocean: Impact of the subsurface chlorophyll maximum on regional, seasonal, and annual primary production estimates. *Biogeosciences* **10**: 4383. doi:10.5194/bg-10-4383-2013
- Ashley, M. C., S. C. Mangi, and L. D. Rodwell. 2014. The potential of offshore windfarms to act as marine protected areas - a systematic review of current evidence. *Mar. Policy* **45**: 301–309. doi:10.1016/j.marpol.2013.09.002
- Åström, E. K. L., M. L. Carroll, W. G. Ambrose, and J. Carroll. 2016. Arctic cold seeps in marine methane hydrate environments: Impacts on shelf macrobenthic community structure offshore Svalbard. *Mar. Ecol. Prog. Ser.* **552**: 1–18. doi:10.3354/meps11773
- Åström, E. K. L., P. G. Oliver, and M. L. Carroll. 2017. A new genus and two new species of Thyasiridae associated with methane seeps off Svalbard, Arctic Ocean. *Mar. Biol. Res.* **13**: 402–416. doi:10.1080/17451000.2016.1272699
- Baine, M. 2001. Artificial reefs: A review of their design, application, management and performance. *Ocean Coast. Manag.* **44**: 241–259. doi:10.1016/S0964-5691(01)00048-5
- Bale, A., and A. Kenny. 2005. Sediment analysis and seabed characterisation, p. 43–87. In A. Eleftheriou and A. McIntyre [eds.], *Methods for the study of marine benthos*. Blackwell Publishing.
- Bergmann, M., T. Soltwedel, and M. Klages. 2011. The inter-annual variability of megafaunal assemblages in the Arctic deep sea: Preliminary results from the HAUSGARTEN observatory (79N). *Deep-Res. Part I Oceanogr. Res. Pap.* **58**: 711–723. doi:10.1016/j.dsr.2011.03.007
- Bernardino, A. F., L. A. Levin, A. R. Thurber, and C. R. Smith. 2012. Comparative composition, diversity and trophic ecology of sediment macrofauna at vents, seeps and organic falls. *PLoS One* **7**: 1–17. doi:10.1371/journal.pone.0033515
- Blazejak, A., C. Erséus, R. Amann, and N. Dubilier. 2005. Coexistence of bacterial sulfide oxidizers, sulfate reducers, and spirochetes in a gutless worm (*Oligochaeta*) from the Peru margin. *Appl. Environ. Microbiol.* **71**: 1553–1561. doi:10.1128/AEM.71.3.1553-1561.2005
- Blazewicz-Paszkowycz, M., and R. N. Bamber. 2011. Tanaidomorph Tanaidacea (Crustacea: Peracarida) from mud-volcano and seep sites on the Norwegian margin. *Zootaxa* **35**: 1–35.
- Bluhm, B. A., and others. 2011. Diversity of the arctic deep-sea benthos. *Mar. Biodivers.* **41**: 87–107. doi:10.1007/s12526-010-0078-4
- Boetius, A., and E. Suess. 2004. Hydrate Ridge: A natural laboratory for the study of microbial life fueled by methane from near-surface gas hydrates. *Chem. Geol.* **205**: 291–310. doi:10.1016/j.chemgeo.2003.12.034
- Boetius, A., and others. 2013. Export of algal biomass from the melting Arctic sea ice. *Science* **339**: 1430–1432. doi:10.1126/science.1231346
- Bohnsack, J. A. 1989. Are high densities of fishes at artificial reefs the result of habitat limitation or behavioral preference? *Bull. Mar. Sci.* **44**: 631–645.
- Bohrmann, G., J. Greinert, E. Suess, and M. Torres. 1998. Authigenic carbonates from the Cascadia subduction zone and their relation to gas hydrate stability. *Geology* **26**: 647–650. doi:10.1130/0091-7613(1998)026<0647:ACFTCS>2.3.CO;2
- Bowden, D. A., A. A. Rowden, A. R. Thurber, A. R. Baco, L. A. Levin, and C. R. Smith. 2013. Cold seep epifaunal communities on the Hikurangi margin, New Zealand: Composition, succession, and vulnerability to human activities. *PLoS One* **8**: 1–20 doi:10.1371/journal.pone.0076869
- Bünz, S., S. Polyakov, S. Vadakkepuliyambatta, C. Consolaro, and J. Mienert. 2012. Active gas venting through hydrate-bearing sediments on the Vestnesa Ridge, offshore W-

- Svalbard. *Mar. Geol.* **332–334**: 189–197. doi:10.1016/j.margeo.2012.09.012
- Buhl-Mortensen, L., P. Buhl-Mortensen, M. F. J. Dolan, J. Dannheim, V. Bellec, and B. Holte. 2012. Habitat complexity and bottom fauna composition at different scales on the continental shelf and slope of northern Norway. *Hydrobiologia* **685**: 191–219. doi:10.1007/s10750-011-0988-6
- Carney, R. S. 1994. Consideration of the oasis analogy for chemosynthetic communities at Gulf of Mexico hydrocarbon vents. *Geo Mar. Lett.* **14**: 149–159. doi:10.1007/BF01203726
- Carney, R. S. 2005. Zonation of deep biota on continental margins. *Oceanogr. Mar. Biol. Annu. Rev.* **43**: 211–278. doi:10.1201/9781420037449.ch6
- Carroll, M. L., S. G. Denisenko, P. E. Renaud, and W. G. Ambrose. 2008. Benthic infauna of the seasonally ice-covered western Barents Sea: Patterns and relationships to environmental forcing. *Deep-Sea Res. Part II Top. Stud. Oceanogr.* **55**: 2340–2351. doi:10.1016/j.dsr2.2008.05.022
- Cathles, L., S. Zheng, and D. Chen. 2010. The physics of gas chimney and pockmark formation, with implications for assessment of seafloor hazards and gas sequestration. *Mar. Pet. Geol.* **27**: 82–91. doi:10.1016/j.marpetgeo.2009.09.010
- Clark, M. R., F. Althaus, T. A. Schlacher, A. Williams, D. A. Bowden, and A. A. Rowden. 2016. The impacts of deep-sea fisheries on benthic communities: A review. *ICES J. Mar. Sci.* **73**: i51–i69. doi:10.1093/icesjms/fsv123
- Clarke, K. R., and R. N. Gorley. 2006. PRIMER V6: User manual-tutorial. Plymouth Marine Laboratory.
- Clough, L. M., W. G. Ambrose, J. K. Cochran, C. Barnes, P. E. Renaud, and R. C. Aller. 1997. Infaunal density, biomass and bioturbation in the sediments of the Arctic Ocean. *Deep-Sea Res. Part II Top. Stud. Oceanogr.* **44**: 1683–1704. doi:10.1016/S0967-0645(97)00052-0
- Cochrane, S. K. J., T. H. Pearson, M. Greenacre, J. Costelloe, I. H. Ellingsen, S. Dahle, and B. Gulliksen. 2012. Benthic fauna and functional traits along a Polar Front transect in the Barents Sea – advancing tools for ecosystem-scale assessments. *J. Mar.* **94**: 204–217. doi:10.1016/j.jmarsys.2011.12.001
- Cordes, E. E., E. L. Becker, S. Hourdez, and C. R. Fisher. 2010. Influence of foundation species, depth, and location on diversity and community composition at Gulf of Mexico lower-slope cold seeps. *Deep-Sea Res. Part II Top. Stud. Oceanogr.* **57**: 1870–1881. doi:10.1016/j.dsr2.2010.05.010
- Crémière, A., and others. 2016. Fluid source and methane-related diagenetic processes recorded in cold seep carbonates from the Alvheim channel, central North Sea. *Chem. Geol.* **432**: 16–33. doi:10.1016/j.chemgeo.2016.03.019
- Dando, P. R., and others. 1991. Ecology of a North Sea pockmark with an active methane seep. *Mar. Ecol. Prog. Ser.* **70**: 49–63. doi:10.3354/meps070049
- Decker, C., M. Morineaux, S. Van Gaever, J. C. Caprais, A. Lichtschlag, O. Gauthier, A. C. Andersen, and K. Olu. 2012. Habitat heterogeneity influences cold-seep macrofaunal communities within and among seeps along the Norwegian margin. Part 1: Macrofaunal community structure. *Mar. Ecol.* **33**: 205–230. doi:10.1111/j.1439-0485.2011.00503.x
- Decker, C., and K. Olu. 2012. Habitat heterogeneity influences cold-seep macrofaunal communities within and among seeps along the Norwegian margin—part 2: Contribution of chemosynthesis and nutritional patterns. *Mar. Ecol.* **33**: 231–245. doi:10.1111/j.1439-0485.2011.00486.x
- Domack, E., S. Ishman, A. Leventer, S. Sylva, V. Willmott, and B. Huber. 2005. A chemotrophic ecosystem found beneath Antarctic Ice Shelf. *Eos Trans. Am. Geophys. Union* **86**: 269–272. doi:10.1029/2005EO290001
- Dubilier, N., C. Bergin, and C. Lott. 2008. Symbiotic diversity in marine animals: The art of harnessing chemosynthesis. *Nat. Rev. Microbiol.* **6**: 725–740. doi:10.1038/nrmicro1992
- Dufour, S. C. 2005. Gill anatomy and the evolution of symbiosis in the bivalve family Thyasiridae. *Biol. Bull.* **208**: 200–212. doi:10.2307/3593152
- Etter, R., and F. Grassle. 1992. Patterns of species diversity in the deep sea as a function of sediment particle size diversity. *Nature* **360**: 576–578. doi:10.1038/360576a0
- Gage, J. D., and P. A. Tyler. 1991. *Deep-sea biology: A natural history of organisms at the deep-sea floor.* Cambridge Univ. Press.
- Gebbruk, A., E. Krylova, A. Lein, G. Vinogradov, E. Anderson, N. Pimenov, G. Cherkashev, and K. Crane. 2003. Methane seep community of the Håkon Mosby mud volcano (the Norwegian Sea) composition and trophic aspects. *Sarsia* **88**: 394–403. doi:10.1080/00364820310003190
- Gentz, T., E. Damm, J. Schneider von Deimling, S. Mau, D. F. McGinnis, and M. Schlüter. 2014. A water column study of methane around gas flares located at the West Spitsbergen continental margin. *Cont. Shelf Res.* **72**: 107–118. doi:10.1016/j.csr.2013.07.013
- Gooday, A. J., C. M. Turley, and J. A. Allen. 1990. Responses by benthic organisms to inputs of organic material to the ocean floor: A review [and discussion]. *Philos. Trans. R. Soc. Lond. A Math. Phys. Eng. Sci.* **331**: 119–138. doi:10.1098/rsta.1990.0060
- Graf, G. 1989. Benthic-pelagic coupling in a deep-sea benthic community. *Nature* **341**: 437–439. doi:10.1038/340301a0
- Hammer, Ø., K. Webb, and D. DePreiter. 2009. Numerical simulation of upwelling currents in pockmarks, and data from the Inner Oslofjord, Norway. *Geo Mar. Lett.* **29**: 269–275. doi:10.1007/s00367-009-0140-z
- Harris, L. D. 1988. Edge effects and conservation of biotic diversity. *Conserv. Biol.* **2**: 330–332. doi:10.1111/j.1523-1739.1988.tb00196.x
- Holm-Hansen, O., C. Lorenzon, R. Holmes, and J. Strickland. 1965. Fluorometric determination of chlorophyll. *ICES J. Mar. Sci.* **30**: 3–15. doi:10.1093/icesjms/30.1.3
- Hong, W.-L., S. Sauer, G. Panieri, W. G. Ambrose, R. H. James, A. Plaza-Faverola, and A. Schneider. 2016. Removal

- of methane through hydrological, microbial, and geochemical processes in the shallow sediments of pockmarks along eastern Vestnesa Ridge (Svalbard). *Limnol. Oceanogr.* **61**: S324–S343. doi:10.1002/lno.10299
- Hoste, E., S. Vanhove, I. Schewe, T. Soltwedel, and A. Vanreusel. 2007. Spatial and temporal variations in deep-sea meiofauna assemblages in the Marginal Ice Zone of the Arctic Ocean. *Deep-Sea Res. Part I Oceanogr. Res. Pap.* **54**: 109–129. doi:10.1016/j.dsr.2006.09.007
- Hovland, M., and A. G. Judd. 1988. The ecology of pockmarks and seepages, p. 227–245. *In* Seabed pockmarks and seepages — impact on geology, biology and the marine environment. Graham & Trotman, London, 293 pp.
- Hovland, M., H. Svensen, C. F. Forsberg, H. Johansen, C. Fichler, J. H. Fosså, R. Jonsson, and H. Rueslåtten. 2005. Complex pockmarks with carbonate-ridges off mid-Norway: Products of sediment degassing. *Mar. Geol.* **218**: 191–206. doi:10.1016/j.margeo.2005.04.005
- Hovland, M., and H. Svensen. 2006. Submarine pingoes: Indicators of shallow gas hydrates in a pockmark at Nyegga, Norwegian Sea. *Mar. Geol.* **228**: 15–23. doi:10.1016/j.margeo.2005.12.005
- Hustoft, S., S. Bünz, J. Mienert, and S. Chand. 2009. Gas hydrate reservoir and active methane-venting province in sediments on <20 Ma young oceanic crust in the Fram Strait, offshore NW-Svalbard. *Earth Planet. Sci. Lett.* **284**: 12–24. doi:10.1016/j.epsl.2009.03.038
- Jakobsson, M., and others. 2012. The International Bathymetric Chart of the Arctic Ocean (IBCAO) version 3.0. *Geophys. Res. Lett.* **39**: 1–6. doi:10.1029/2012GL052219
- Johnson, J. E., J. Mienert, A. Plaza-Faverola, S. Vadakkepuliambatta, J. Knies, S. Bünz, K. Andreassen, and B. Ferré. 2015. Abiotic methane from ultraslow-spreading ridges can charge Arctic gas hydrates. *Geology* **43**: 371–374. doi:10.1130/G36440.1
- Krönke, I. 1998. Macrofauna communities in the Amundsen Basin, at the Morris Jesup Rise and at the Yermak Plateau (Eurasian Arctic Ocean). *Polar Biol.* **19**: 383–392. doi:10.1007/s003000050263
- Lammers, S., E. Suess, and M. Hovland. 1995. A large methane plume east of Bear Island (Barents Sea): Implications for the marine methane cycle. *Geol. Rundsch.* **84**: 59–66. doi:10.1007/BF00192242
- Lein, A., P. Vogt, K. Crane, A. Egorov, and M. Ivanov. 1999. Chemical and isotopic evidence for the nature of the fluid in CH₄-containing sediments of the Håkon Mosby Mud Volcano. *Geo Mar. Lett.* **19**: 76–83. doi:10.1007/s003670050095
- Levin, L. A. 2005. Ecology of cold seep sediments: Interactions of fauna with flow, chemistry and microbes. *Oceanogr. Mar. Biol.* **43**: 1–46. doi:10.1201/9781420037449.ch1
- Levin, L. A., and others. 2001. Environmental influences on regional deep-sea species diversity source. *Annu. Rev. Ecol. Syst.* **132**: 51–93. doi:10.1146/annurev.ecolsys.32.081501.114002
- Levin, L. A., and R. H. Michener. 2002. Isotopic evidence for chemosynthesis-based nutrition of macrobenthos: The lightness of being at Pacific methane seeps. *Limnol. Oceanogr.* **47**: 1336–1345. doi:10.4319/lo.2002.47.5.1336
- Levin, L. A., and others. 2016. Hydrothermal vents and methane seeps: Rethinking the sphere of influence. *Front. Mar. Sci.* **3**: 72. doi:10.3389/fmars.2016.00072
- Livingston, B. E. 1903. The distribution of the upland plant societies of Kent County, Michigan. *Bot. Gaz.* **35**: 36–55. doi:10.1086/328315
- Lösekann, T., A. Robador, H. Niemann, K. Knittel, A. Boetius, and N. Dubilier. 2008. Endosymbioses between bacteria and deep-sea siboglinid tubeworms from an Arctic Cold Seep (Haakon Mosby Mud Volcano, Barents Sea). *Environ. Microbiol.* **10**: 3237–3254. doi:10.1111/j.1462-2920.2008.01712.x
- MacDonald, I. R., B. A. Bluhm, K. Iken, S. Gagaev, and S. Strong. 2010. Benthic macrofauna and megafauna assemblages in the Arctic deep-sea Canada Basin. *Deep-Sea Res. Part II Top. Stud. Oceanogr.* **57**: 136–152. doi:10.1016/j.dsr2.2009.08.012
- Meunier, C., A. C. Andersen, M. Bruneaux, D. Le Guen, P. Terrier, E. Leize-Wagner, and F. Zal. 2010. Structural characterization of hemoglobins from Monilifera and Frenulata tubeworms (Siboglinids): First discovery of giant hexagonal-bilayer hemoglobin in the former “Pogonophora” group. *Comp. Biochem. Physiol. A Mol. Integr. Physiol.* **155**: 41–48. doi:10.1016/j.cbpa.2009.09.010
- Meyer, K. S., M. Bergmann, and T. Soltwedel. 2013. Interannual variation in the epibenthic megafauna at the shallowest station of the HAUSGARTEN observatory (79°N, 6°E). *Biogeosciences* **10**: 3479–3492. doi:10.5194/bg-10-3479-2013
- Meyer, K. S., T. Soltwedel, and M. Bergmann. 2014. High biodiversity on a deep-water reef in the eastern Fram Strait. *PLoS One* **9**: 1–16. doi:10.1371/journal.pone.0105424
- Milkov, A., P. Vogt, G. Cherkashev, G. Ginsburg, N. Chernova, and A. Andriashev. 1999. Sea-floor terrains of Hakon Mosby Mud Volcano as surveyed by deep-tow video and still photography. *Geo Mar. Lett.* **19**: 38–47. doi:10.1007/s003670050091
- Niemann, H., and others. 2013. Methane-carbon flow into the benthic food web at cold seeps - a case study from the Costa Rica subduction zone. *PLoS One* **8**: 4–13. doi:10.1371/journal.pone.0074894
- Olu, K., and others. 2009. Influence of seep emission on the non-symbiont-bearing fauna and vagrant species at an active giant pockmark in the Gulf of Guinea (Congo-Angola margin). *Deep-Sea Res. Part II Top. Stud. Oceanogr.* **56**: 2380–2393. doi:10.1016/j.dsr2.2009.04.017
- Olu, K., E. E. Cordes, C. R. Fisher, J. M. Brooks, M. Sibuet, and D. Desbruyères. 2010. Biogeography and potential exchanges among the Atlantic equatorial belt cold-seep faunas. *PLoS One* **5**: 1–11. doi:10.1371/journal.pone.0011967
- Paul, A., and R. Menzies. 1974. Benthic ecology of the high arctic deep sea. *Mar. Biol.* **27**: 251–262. doi:10.1007/BF00391950

- Payne, C. M., and J. A. Allen. 1991. The morphology of deep-sea Thyasiridae (Mollusca: Bivalvia) from the Atlantic Ocean. *Philos. Trans. R. Soc. Lond. B Biol. Sci.* **334**: 481–562. doi:10.1098/rstb.1991.0128
- Piepenburg, D., V. N. Chernova, F. C. von Dorrien, J. Gutt, V. A. Neyelov, E. Rachor, L. Saldanha, and K. M. Schmid. 1996. Megabenthic communities in the waters around Svalbard. *Polar Biol.* **16**: 431–446. doi:10.1007/BF02390425
- Piepenburg, D., and M. K. Schmid. 1996. Brittle star fauna (Echinodermata: Ophiuroidea) of the Arctic northwestern Barents Sea: Composition, abundance, biomass and spatial distribution. *Polar Biol.* **16**: 383–392. doi:10.1007/BF02390420
- Piepenburg, D., and others. 2011. Towards a pan-Arctic inventory of the species diversity of the macro- and megabenthic fauna of the Arctic shelf seas. *Mar. Biodivers.* **41**: 51–70. doi:10.1007/s12526-010-0059-7
- Plaza-Faverola, A., S. Bünz, J. E. Johnson, S. Chand, J. Knies, J. Mienert, and P. Franek. 2015. Role of tectonic stress in seepage evolution along the gas hydrate-charged Vestnesa Ridge, Fram Strait. *Geophys. Res. Lett.* **42**: 733–742. doi:10.1002/2014GL062474
- Pleijel, F., T. G. Dahlgren, and G. W. Rouse. 2009. Progress in systematics: From Siboglinidae to Pogonophora and Vestimentifera and back to Siboglinidae. *C. R. Biol.* **332**: 140–148. doi:10.1016/j.crv.2008.10.007
- Quéric, N. V., and T. Soltwedel. 2007. Impact of small-scale biogenic sediment structures on bacterial distribution and activity in Arctic deep-sea sediments. *Mar. Ecol.* **28**: 66–74. doi:10.1111/j.1439-0485.2007.00177.x
- Rehder, G., R. S. Keir, E. Suess, and M. Rhein. 1999. Methane in the northern Atlantic controlled by microbial oxidation and atmospheric history. *Geophys. Res. Lett.* **26**: 587–590. doi:10.1029/1999GL900049
- Renaud, P. E., M. Włodarska-Kowalczyk, H. Trannum, B. Holte, J. Marcin Weslawski, S. Cochrane, S. Dahle, and B. Gulliksen. 2007. Multidecadal stability of benthic community structure in a high-Arctic glacial fjord (van Mijenfjord, Spitsbergen). *Polar Biol.* **30**: 295–305. doi:10.1007/s00300-006-0183-9
- Rex, M. A. 1981. Structure in community the deep-sea benthos. *Annu. Rev. Ecol. Syst.* **12**: 331–353. doi:10.1146/annurev.es.12.110181.001555
- Rice, A. L., D. S. M. Billett, J. Fry, A. W. G. John, R. S. Lampitt, R. F. C. Mantoura, and R. J. Morris. 1985. Seasonal deposition of phytodetritus to the deep-sea floor. *Proc. R. Soc. Edinb. Sect. B Biol. Sci.* **88**: 265–279. doi:10.1017/S0269727000004590
- Ritt, B., C. Pierre, O. Gauthier, F. Wenzhöfer, A. Boetius, and J. Sarrazin. 2011. Diversity and distribution of cold-seep fauna associated with different geological and environmental settings at mud volcanoes and pockmarks of the Nile Deep-Sea Fan. *Mar. Biol.* **158**: 1187–1210. doi:10.1007/s00227-011-1679-6
- Rudels, B., R. Meyer, E. Fahrbach, V. V. Ivanov, and D. Quadfasel. 2000. Water mass distribution in Fram Strait and over the Yermak Plateau in summer 1997. *Ann. Geophys.* **18**: 687–705. doi:10.1007/s00585-000-0687-5
- Rybakova, E., S. Galkin, M. Bergmann, T. Soltwedel, and A. Gebruk. 2013. Density and distribution of megafauna at the Håkon Mosby mud volcano (the Barents Sea) based on image analysis. *Biogeosciences* **10**: 3359–3374. doi:10.5194/bg-10-3359-2013
- Sakshaug, E. 2004. Primary and secondary production in the Arctic Seas, p. 57–81. *In* R. Stein [ed.], *The organic carbon cycle in the Arctic Ocean*. Springer-Verlag.
- Sanders, H. L., and R. R. Hessler. 1969. Ecology of the deep-sea benthos. *Science* **163**: 1419–1424. doi:10.1126/science.163.3874.1419
- Schulz, M., M. Bergmann, K. von Juterzenka, and T. Soltwedel. 2010. Colonisation of hard substrata along a channel system in the deep Greenland Sea. *Polar Biol.* **33**: 1359–1369. doi:10.1007/s00300-010-0825-9
- Sellanes, J., E. Quiroga, and C. Neira. 2008. Megafauna community structure and trophic relationships at the recently discovered Concepción Methane Seep Area Chile, ~36° S. *ICES J. Mar. Sci.* **65**: 1102–1111. doi:10.1093/icesjms/fsn099
- Sellanes, J., G. Zapata-Hernández, S. Pantoja, and G. L. Jessen. 2011. Chemosynthetic trophic support for the benthic community at an intertidal cold seep site at Mocha Island off central Chile. *Estuar. Coast. Shelf Sci.* **95**: 431–439. doi:10.1016/j.ecss.2011.10.016
- Sen, A., S. Kim, A. J. Miller, K. J. Hovey, S. Hourdez, G. W. Luther, and C. R. Fisher. 2016. Peripheral communities of the Eastern Lau Spreading Center and Valu Fa Ridge: Community composition, temporal change and comparison to near-vent communities. *Mar. Ecol.* **37**: 599–617. doi:10.1111/maec.12313
- Smith, A. J., J. Mienert, S. Bünz, and J. Greinert. 2014. Thermogenic methane injection via bubble transport into the upper Arctic Ocean from the hydrate-charged Vestnesa Ridge, Svalbard. *Geochem. Geophys. Geosyst.* **15**: 1945–1959. doi:10.1002/2013GC005179
- Solheim, A., and A. Elverhøi. 1993. Gas-related sea floor craters in the Barents Sea. *Geo Mar. Lett.* **13**: 235–243. doi:10.1007/BF01207753
- Soltwedel, T., N. Jaekisch, N. Ritter, C. Hasemann, M. Bergmann, and M. Klages. 2009. Bathymetric patterns of megafaunal assemblages from the arctic deep-sea observatory HAUSGARTEN. *Deep-Sea Res. Part I Oceanogr. Res. Pap.* **56**: 1856–1872. doi:10.1016/j.dsr.2009.05.012
- Soltwedel, T., and others. 2015. Natural variability or anthropogenically-induced variation? Insights from 15 years of multidisciplinary observations at the arctic marine LTER site HAUSGARTEN. *Ecol. Indic.* **65**: 89–102. doi:10.1016/j.ecolind.2015.10.001

- Søreide, J. E., H. Hop, M. L. Carroll, S. Falk-Petersen, and E. N. Hegseth. 2006. Seasonal food web structures and sympagic–pelagic coupling in the European Arctic revealed by stable isotopes and a two-source food web model. *Prog. Oceanogr.* **71**: 59–87. doi:10.1016/j.pocean.2006.06.001
- Sorokin, Y. I., P. Y. Sorokin, and O. Y. Zakouskina. 2003. Microplankton and its function in a zone of shallow hydrothermal activity: The Craternaya Bay, Kurile Islands. *J. Plankton Res.* **25**: 495–506. doi:10.1093/plankt/25.5.495
- Southward, A. J., and E. C. Southward. 1982. The role of dissolved organic matter in the nutrition of deep-sea benthos. *Am. Zool.* **22**: 647–658. doi:10.1093/icb/22.3.647
- Stone, R. B., H. L. Pratt, R. O. Parker, and G. E. Davis. 1979. A comparison of fish populations on an artificial and natural reef in the Florida Keys. *Mar. Fish. Rev.* **41**: 1–11.
- Sztybor, K., and T. L. Rasmussen. 2016. Diagenetic disturbances of marine sedimentary records from methane-influenced environments in the Fram Strait as indications of variation in seep intensity during the last 35 000 years. *Boreas.* **46**: 212–228. doi:10.1111/bor.12202
- Tarasov, V. G., A. V. Gebruk, A. N. Mironov, and L. I. Moskalev. 2005. Deep-sea and shallow-water hydrothermal vent communities: Two different phenomena? *Chem. Geol.* **224**: 5–39. doi:10.1016/j.chemgeo.2005.07.021
- Taylor, J., T. Krumpen, T. Soltwedel, J. Gutt, and M. Bergmann. 2016. Regional- and local-scale variations in benthic megafaunal composition at the Arctic deep-sea observatory HAUSGARTEN. *Deep-Sea Res. Part I Oceanogr. Res. Pap.* **108**: 58–72. doi:10.1016/j.dsr.2015.12.009
- Taylor, J. D., and E. A. Glover. 2010. Chemosymbiotic bivalves, p. 107–135. *In* S. Kiel [ed.], *The vent and seep biota*. Springer.
- Thurber, A. R., L. A. Levin, A. A. Rowden, S. Sommer, P. Linke, and K. Kröer. 2013. Microbes, macrofauna, and methane: A novel seep community fueled by aerobic methanotrophy. *Limnol. Oceanogr.* **58**: 1640–1656. doi:10.4319/lo.2013.58.5.1640
- Vanreusel, A., L. Clough, K. Jacobsen, W. Ambrose, V. Ryheul, R. Herman, and M. Vincx. 2000. Meiobenthos of the central Arctic Ocean with special emphasis on the nematode community structure. *Deep-Sea Res. Part I Oceanogr. Res. Pap.* **47**: 1855–1856. doi:10.1016/S0967-0637(00)00007-8
- Vanreusel, A., and others. 2009. Biodiversity of cold seep ecosystems along the European margins. *Oceanography* **22**: 110–127. doi:10.5670/oceanog.2009.12
- Vedenin, A., N. Budaeva, V. Mokievsky, C. Pantke, T. Soltwedel, and A. Gebruk. 2016. Spatial distribution patterns in macrobenthos along a latitudinal transect at the deep-sea observatory HAUSGARTEN. *Deep-Sea Res. Part I Oceanogr. Res. Pap.* **114**: 90–98. doi:10.1016/j.dsr.2016.04.015
- Vismann, B. 1991. Sulfide tolerance: Physiological mechanisms and ecological implications. *Ophelia* **34**: 1–27.
- Vogt, P., K. Crane, E. Sundvor, M. D. Max, and S. L. Pfirman. 1994. Methane-generated(?) pockmarks on young, thickly sedimented oceanic crust in the Arctic: Vestnesa Ridge, Fram Strait. *Geology* **22**: 255–258. doi:10.1130/0091-7613(1994)022<0255:MGPOYT>2.3.CO;2
- Vogt, P. R., and others. 1997. Haakon Mosby Mud Volcano provides unusual example of venting. *EOS Trans. Am. Geophys. Union* **78**: 549–557. doi:10.1029/97EO00326
- Warwick, R. M., and K. R. Clarke. 1995. New “biodiversity” measures reveal a decrease in taxonomic distinctness with increasing stress. *Mar. Ecol. Prog. Ser.* **129**: 301–305. doi:10.3354/meps129301
- Wassmann, P., and M. Reigstad. 2011. Future Arctic Ocean seasonal ice zones and implications for pelagic-benthic coupling. *Oceanography* **24**: 220–231. doi:10.5670/oceanog.2011.74
- Webb, K., D. K. A. Barnes, and J. S. Gray. 2009a. Benthic ecology of pockmarks in the Inner Oslofjord, Norway. *Mar. Ecol. Prog. Ser.* **387**: 15–25. doi:10.3354/meps08079
- Webb, K., D. K. A. Barnes, and S. Planke. 2009b. Pockmarks: Refuges for marine benthic biodiversity. *Limnol. Oceanogr.* **54**: 1776–1788. doi:10.4319/lo.2009.54.5.1776
- Westbrook, G. K., and others. 2009. Escape of methane gas from the seabed along the West Spitsbergen continental margin. *Geophys. Res. Lett.* **36**: 1–5. doi:10.1029/2009GL039191
- Wheeler, P. A., M. Gosselin, E. Sherr, D. Thibault, D. L. Kirchman, R. Benner, and T. E. Whittledge. 1996. Active cycling of organic carbon in the central Arctic Ocean. *Nature* **380**: 697–699. doi:10.1038/380697a0
- Wiesenburg, D. A., and L. J. Guinasso. 1979. Equilibrium solubilities of methane, in water and sea water. *J. Chem. Eng. Data.* **24**: 356–360 doi:10.1021/je60083a006
- Wilson, J. C., and M. Elliott. 2009. The habitat-creation potential of offshore wind farms. *Wind Energy* **12**: 203–212. doi:10.1002/we.324
- Włodarska-Kowalczyk, M., M. A. Kendall, J. Marcin Weslawski, M. Klages, and T. Soltwedel. 2004. Depth gradients of benthic standing stock and diversity on the continental margin at a high-latitude ice-free site (off Spitsbergen, 79N). *Deep-Sea Res. Part I Oceanogr. Res. Pap.* **51**: 1903–1914. doi:10.1016/j.dsr.2004.07.013
- Włodarska-Kowalczyk, M., and T. H. Pearson. 2004. Soft-bottom macrobenthic faunal associations and factors affecting species distributions in an Arctic glacial fjord (Kongsfjord, Spitsbergen). *Polar Biol.* **27**: 155–167. doi:10.1007/s00300-003-0568-y
- Włodarska-Kowalczyk, M., P. E. Renaud, J. Marcin Weslawski, S. K. J. Cochrane, and S. G. Denisenko. 2012. Species diversity, functional complexity and rarity in Arctic fjordic versus open shelf benthic systems. *Mar. Ecol. Prog. Ser.* **463**: 73–87. doi:10.3354/meps09858
- Zaborska, A., J. Carroll, C. Papucci, L. Torricelli, M. L. Carroll, J. Walkusz-Miotk, and J. Pempkowiak. 2008.

Recent sediment accumulation rates for the Western margin of the Barents Sea. *Deep-Sea Res. Part II Top. Stud. Oceanogr.* **55**: 2352–2360. doi:[10.1016/j.dsr2.2008.05.026](https://doi.org/10.1016/j.dsr2.2008.05.026)
Zeppilli, D., M. Canals, and R. Danovaro. 2012. Pockmarks enhance deep-sea benthic biodiversity: A case study in the western Mediterranean Sea. *Divers. Distrib.* **18**: 832–846. doi:[10.1111/j.1472-4642.2011.00859.x](https://doi.org/10.1111/j.1472-4642.2011.00859.x)

Acknowledgments

We acknowledge the captain and crew of RV “*Helmer Hanssen*” and the scientific teams from CAGE 14_1 and CAGE 15_2 cruises. Also thanks to D. Fornari at Woods Hole Oceanographic Institute (WHOI) and the Multidisciplinary Instrumentation in Support of Oceanography, (MISO) USA for the collaboration with CAGE in developing the TOW-camera system. Thanks to sorters and taxonomic specialists at the biological laboratory at Akvaplan-niva, Tromsø, for processing samples. We are grateful for the work of A. Portnov for Fig. 1, A. Plaza-Faverola in processing the seismic data for Fig. 2, D. Hammenstig for assistance and edits of photos and to K. Waghorn and P. Serov for discussions about the geological history of the region, sources of methane and sub-seabed

features. We are also thankful to three anonymous reviewers for perceptive comments that helped refine the final manuscript. W.G.A. was an employee of the US NSF at the time this work was conducted; however, any opinions, findings, conclusions, or recommendations expressed in this material are those of W.G.A. and his co-authors, and do not necessarily reflect the views of the US NSF. The seabed images are stored at the CAGE data repository and more information is available by contacting the responsible author or data manager at CAGE (<https://cage.uit.no/>). This work was funded through the Centre for Arctic Gas Hydrate, Environment and Climate (CAGE) and the Research Council of Norway through its Centers’ of Excellence funding scheme, project number 223259.

Conflict of Interest

None declared.

Submitted 06 April 2017

Revised 26 June 2017

Accepted 14 September 2017

Associate editor: Leila Hamdan